# ECC Report 262

Studies related to surveillance radar equipment operating in the 76 to 77 GHz range for fixed transport infrastructure

**Approved 27 January 2017**

# 0 EXECUTIVE SUMMARY

This study has concentrated on radars using FMCW technology since those are the only examples made known to ECC during the course of the study.

For this study only one particular example of a fixed radar application has been investigated. This particular application has a main-beam peak Tx-Power of 39 dBm e.i.r.p., a detection range of ≤ 500m, a rotation frequency between 1 Hz and 4 Hz combined with 1.8° beamwidth at the 3 dB point and was tested at a mounting height of 4m (see details in [1]).

On the automotive side, two examples of front looking radar sensors and one example of rear-side looking radar sensors from three different manufacturers have been investigated in this study. These have some features in common like using a kind of FMCW modulation or using a focussed antenna characteristics in elevation. But driven by different application requirements they differ in other features like transmit power, modulation bandwidth, antenna azimuth beamwidth or receive signal processing algorithms. More details on automotive radar sensors in general can be found for example in Recommendation ITU-R M.2057 [2] or in Handbook of Driver Assistance Systems [3].

This report has investigated scenarios with only one victim and one interfering sensor in an open area under ideal environmental conditions. The simulations are based on those assumptions.

This study analysed the impact:

- of one fixed infrastructure radar mounted at roadside installations used for road traffic monitoring onto automotive radar used for vehicle traffic safety and comfort functions and;
- automotive radars onto fixed infrastructure radar used for road traffic monitoring.

The study did not however investigate any impact of fixed infrastructure radar to fixed infrastructure radar systems or automotive radar to automotive radar systems.

The analysis was done based on

- detailed information on 3 different automotive radar systems from 3 different suppliers (Automotive Radar Systems A,B,C);
- detailed information on one fixed infrastructure radar system from one manufacturer;
- cooperative and organised experimental "open area" tests on the Neuhausen/Germany air field in a 1test campaign simulating typical roadside installation on highways (outside tunnels);
- simulations to verify the "open area" test results using a simulator based on the MCL (minimum coupling loss) method on spread sheet basis, developed during this work item.

In addition, two suppliers of automotive radar (systems A and C) independently tested the impact of an installation of 6 fixed radars deployed in the Hindhead/UK tunnel onto their automotive radar.

Both theoretical analysis and practical results show that the effect of any single FMCW radar on another operating at the same frequency is a raising of the post processing noise floor. This effect is the dominant one providing there is no accidental synchronisation between the two radars, which could increase the probability to detect ghost target. Due to movement of vehicles and scanning of fixed radar, the noise floor raising varies with time.

Establishing the exact degree by which the noise floor is raised and the overall effect on the radar is not straightforward. The theoretical model is the subject of debate and research; practical measurements are subject to a number of limitations. The following points, however, have been established:

1 The increases in noise floor (either calculated or observed) seen in this study can, be in the order of 10 dB or equivalent to a reduction of 45% detection range during an affected measurement cycle from a fixed infrastructure radar operating at 39 dBm, in certain scenarios based on particular radars and relative heights between radars.

2 Possibility of the noise floor increase depends on the probability of two or more systems with independent sweep parameters, scanning rate, occupied bandwidth and duty cycles illuminating each other during their transmit and receive period.

If a single typical vehicle radar passes a typical roadside infrastructure radar, then both radars will receive energy that may affect their operation.

The incident power received by the victim automotive radar from a fixed radar studied in this report at its antenna feed point can be of the same order of magnitude as the power received from a second automotive radar.

The simulation tool only calculates incident power levels at the victim's receiver antenna. Incident power alone does not directly transfer into interference. Incident power is only one aspect of interference being generated in the receiver. The simulation tool does not consider any system level or mitigation aspects beyond the receive antenna such as e.g. occupied bandwidth, frequency hopping, duty cycling.

The technical analysis in this report was set out to investigate worst case conditions for interference between the two radar applications in an open area roadside scenario. The analysis is not, however, representative of all real life installations.

Measurements and calculations from the limited analysis set out in Section 3 of this report suggest that:

- The impact of fixed radar onto automotive radar in open area is a transient (intermittent) and periodic 5-10 dB noise increase, resulting in a decreased sensitivity of the vehicle radar beyond the limit proposed by Recommendation ITU-R M.2057 [2]. This effect may appear above the system noise floor-level of automotive radars based on the probability of two or more systems with independent sweep parameters, scanning rate, occupied bandwidth and duty cycles illuminating each other during their transmit and receive period;
- The impact of automotive radars onto the fixed infrastructure radars in an open area is a transient (intermittent) and periodic noise increase. This may result in a decreased sensitivity of the fixed infrastructure radar in a given azimuth;
- With some evidence of increased impact in tunnels over open road scenarios, the exact effects could not be thoroughly studied due to missing propagation models.

However, with variations in radar types and specifications for both automotive and fixed radars, as well as variations in environmental layout, different simulation results could be reached.

The results of the analysis are detailed in the report in table 0 below. However, recognising the limited analysis done and the fact that the test set-up conditions affect the coexistence, the correct approach to any further analysis needs to be considered carefully.

In summary, this report shows that, the scanning nature of the fixed installation radar contributes to the co-existence with automotive radars, as an interference mitigation method by:

- limitation in the illumination time as seen from a given point in space by the victim radar to ≤ 1,25 ms every 250 ms and ≤ 5 ms every 1000 ms, and;
- a silent time for undisturbed detection by automotive radar systems of no less than 240 ms every 250 ms. This can be achieved by limiting the re-visit time of the illumination.

The values above may need further consideration to take into account the different parameters.

**Table 1: Factors affecting coexistence between automotive and fixed scanning radars**

| Positive effect | Paragraph in the report |
|---|---|
| Small beamwidth of fixed scanning radar (Resulting in lower mean e.i.r.p.) | 2.4.2 |
| High Lateral and vertical separation of fixed scanning radar | 4.2 (may require further study) |
| Appropriate quality of silence time to reduce quasi-synchronous interference | 7.1.2 |
| Appropriate amount of silence time to ensure correct received signals by the automotive radar (Rotation of the fixed scanning radar) | 7.5 (may require further study) |
| Sector Blanking | 8 (may require further study) |
| **Negative effect** | **Paragraph in the report** |
| Reflections (e.g. in tunnels, weather conditions) | 6.2.4 (may require further study) |
| Number of interferers (only one interferer was studied in this report) | (may require further study) |

Finally, without known propagation models for road tunnels, it has not been possible to make an accurate prediction for compatibility. Therefore, further studies may be required before finally concluding on the tunnel case.

During the study it became apparent that the issues raised were far more complex than had been envisaged within the scope of this work item, which included differing vehicular radar types and implementations, different fixed radar mounting positions and configurations. This meant that conventional interference analysis was not considered possible.

## TABLE OF CONTENTS

# LIST OF ABBREVIATIONS

| Abbreviation | Explanation |
|---|---|
| **2D** | Two dimensional |
| **ADC** | Analogue to digital converter |
| **AZ** | Azimuth |
| **BW** | Bandwidth |
| **CEPT** | European Conference of Postal and Telecommunications Administrations |
| **CFAR** | Constant false alarm rate |
| **CMOS** | Complementary metal oxide semiconductor |
| **CTS** | CTS350 Navtech Automatic Incident Detection Radar |
| **ECC** | Electronic Communications Committee |
| **e.i.r.p.** | Equivalent isotropic radiated power |
| **ETSI** | European Telecommunications Standards Institute |
| **FFT** | Fast Fourier transform |
| **FMCW** | Frequency Modulated Continuous Wave (radar) |
| **FOD** | Foreign Object Debris |
| **FOV** | Field of view |
| **FSR** | Fixed Scanning Radar |
| **IF** | Intermediate frequency |
| **I/N** | Interference to noise |
| **ITU** | International Telecommunication Union |
| **LRR** | Long Range Radar |
| **MCL** | Minimum Coupling Loss |
| **MMIC** | Monolithic microwave integrated circuit |
| **MRR** | Medium Range Radar |
| **OB** | Outside Broadcasting |
| **RF** | Radio frequency |
| **RSSI** | Received Signal Strength Indicator: the received power across the whole band |
| **RTTT** | Road transport and traffic telematics |
| **Rx** | Receiver |
| **SEAMCAT** | Spectrum Engineering Advanced Monte Carlo Analysis Tool |
| **S/N** | Signal to noise ratio |
| **SRD** | Short Range Device |
| **SRR** | Short Range Radar |

| Abbreviation | Explanation |
|---|---|
| **TRP** | Total Radiated Power |
| **TTT** | Transport and Traffic Telematics |
| **Tx** | Transmitter |
| **VCO** | Voltage-controlled oscillator |

# 1 INTRODUCTION

This report presents the results of the compatibility studies performed on the sharing of automotive radars operating in the 76 to 77 GHz range with the fixed surveillance radar equipment used for fixed transport infrastructure in accordance with ETSI TR 103 148 [1] operating in the same band.

In the last 10 years, the relevant regulation for the 76-77 GHz band was amended and revised several times. Initially the band 76-77 GHz was designated to automotive radars and RTTT applications this was reflected in ERC/REC 70-03 [4]. In subsequent revisions of ERC/REC 70-03 RTTT applications were removed and later inserted again.

In the context of the 5th update of the SRD decision (2013/752/EU) [5] the scope of the RTTT category was broadened to “Transport and Traffic Telematics systems” (TTT). Following this decision, the entry for the frequency band 76-77 GHz in Annex 5 of ERC/REC 70-03 was revised accordingly.

The vast majority of automotive radars operating in the 76-77 GHz band use an FMCW architecture with only a small percentage using a spread spectrum architecture. The same is true for fixed transport infrastructure radars. Therefore, this report considers only the case of sharing between FMCW automotive radars and FMCW fixed transport infrastructure radars. The impact of fixed transport infrastructure radars on the other radio systems is not considered in this report.

Both automotive radars and fixed transport infrastructure radars operating in the band 76-77 GHz band are covered by the European Commission’s SRD Decision on an equal basis. The set of usage conditions for the SRD category TTT in this decision is available to ground-based vehicle and infrastructure systems. Today, there is no exhaustive information about sharing between the two applications and this report is aimed at filling this gap.

It can be foreseen that under the TTT definition, other potential applications, using the 76-77 GHz radars, would be feasible and that could have an influence on both automotive and fixed transport infrastructure radars (e.g. parking lot monitoring, applications in harbours, etc.). These applications are not considered in the studies included in this report.

This report considers only one type of scanning radar from one manufacturer for fixed transport infrastructure, where the transmit and receiver antennas create a narrow beam which rotates rapidly. Other types (including non-rotating digital beamforming radars) may be available on the market, however they are not considered because of lack of information.

It has to be noted that - as opposed to communications systems - radar sensors do not use standardized signals and standardized signal processing. That makes interference studies more difficult. Even more difficult is the situation here because radar sensors of more than one manufacturer and sometimes more than one sensor generation per manufacturer have to be considered. As a result, the study could not go deep into all technical details. Some parts therefore remain informative.

# 2 FMCW RADARS IN THE 76-77 GHZ BAND

## 2.1 GENERAL

Compared to other radar concepts, FMCW radars offer a good ratio between detection performance and system complexity.

FMCW radars have been under consideration and development for more than 80 years for civil and military applications in a number of different frequency ranges.

FMCW automotive radars, operating in 76-77 GHz band, have been in development for the last 33 years and were initially deployed as adaptive cruise control comfort function by a number of manufacturers. Recent applications include automatic emergency braking, semi-autonomous driving and other safety related functions.

Early developments were made using discrete component structures on quartz substrates and were based on waveguide Gunn diode semiconductor sources. Current products are made using integrated millimetre wave components mounted on ceramic / PTFE composite substrates and are based on synthesized or phase locked sources.

Recent progress in the ratio between performance and price for digital signal processing allowed to further improve radar performance by implementation of more extreme modulation schemes (fast chirp modulation) and advanced analysis strategies (2D or 3D FFT, …) also in price-sensitive automotive products.

As with all radio devices, interference can happen to the receive signal of a FMCW radar if another transmitter is active in the victim receiver's bandwidth. But compared to ultra-wideband pulsed radar sensors, FMCW radar sensors have a very narrow receiver bandwidth compared to their modulation range and are thus more robust. Additionally, interference mitigation techniques like "Constant false alarm rate with adaptive detection threshold" or "Detect interference and change frequency range" or "Detect interference and repair time domain signal" are known and used depending on the available computational resources inside the radar sensor.

This experience was replicated in many military programs of the period, due to the wide deployment of fast sweep FMCW fusing radars for anti-armour applications. Sweep rates used were as fast as any of those proposed for current automotive applications. Both cruise control and fusing radars were deployed in large numbers in critical environments and systems went into production in both areas. Therefore respective countermeasures were taken.

Today there are roughly 10 manufacturers of 77 GHz automotive radars worldwide, and most European and American car manufacturer offers vehicles with one or more such radars as options or as standard. Some vehicles have 5 such radars on board, operating simultaneously. Similar radars are also used in trucks.

## 2.2 FMCW RADAR OPERATING PRINCIPLES

This report adopts an approach to sharing studies between automotive radars and fixed transport infrastructure radars that combines theoretical analysis and practical measurements.

For the analysis the simplified victim receiver topology shown in Figure 1 is assumed.

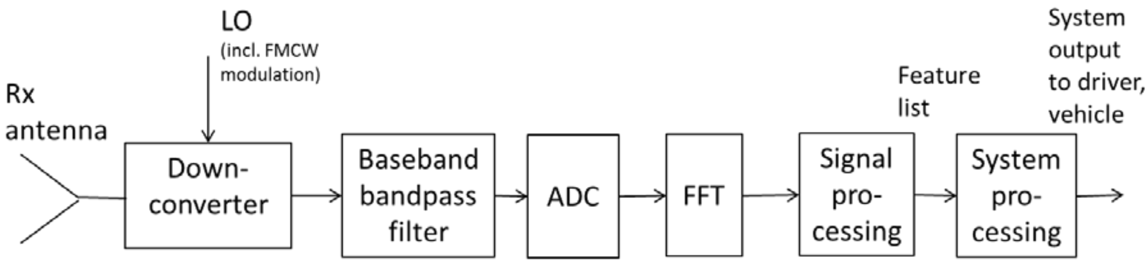


**Figure 1: Assumed, simplified victim receiver topology**

In order to gather intelligence on the position or velocity of a target, some form of modulation is required. A CW signal transmitted into space gives no information regarding a stationary target, other than the change in phase of the reflected signal at the detecting receiver. As the signal is of the form X = Azimuth then if the detected phase changes by ¼ wavelength at the operational frequency, then we know the target or radar has moved by that distance.

As the action is symmetrical – moving the radar or the target gives an identical result for the same distance, then obviously changing the frequency in a linear way must give the same result. As shown in the figure contained in Annex 6, as we know that the speed of light in a fixed dielectric medium such as air, is pretty constant, then this can be used to measure target distance.

If we have a purely CW signal, we have a fixed phase that varies sinusoidally with distance. However if the target is moving at a constant velocity then this rate of change of received phase with respect to time can be used to define that velocity magnitude – the Doppler effect.

With a simple pulse radar we transmit a short burst of radio frequency and use that time of transit, out and back to measure the distance, again assuming the speed of light C = constant. This is a truncated burst of a fixed frequency, and the shorter that pulse then the more accurately we can define the target position. As light speed = 3 x 108 m/s then the narrower the pulse, the shorter range that can be resolved. A 6.6ns pulse can resolve a difference in distance of 1m.

By the same token, we can transform that pulse width to an equivalent frequency deviation, using a Fourier transform. If we transmit a sweep of 1000 MHz/1ms, that is equivalent to 1 x 1012 Hz/s. So if the distance to the target and back is 100 m, then Tr = 0.66ɥs and 0.66ɥs x 1 x 1012 Hz/s = 660 kHz, the distance the source has moved and the range beat frequency that will be seen in the receiver baseband.

We can see that this gives the FMCW radar some fundamental advantages over the pulse radar – firstly by using a frequency sweep the average power is kept very high- pulse radars require very high peak powers in order receive back sufficient average power from a distant target. And by using a high rate of change of frequency, then the ability of non - coherent interfering signals to produce a problem is much reduced. The pulse radar with its fixed frequency local oscillator is vulnerable to any signal that can produce a product signal that falls within its IF, in particular if the interfering signal has the same relative coherence as the stationary LO. Then the transfer of the interfering signal is at the same level set by the conversion loss as its own signals are.

Pulse radars depend on the fact that the temporal coherence is poor between pulse systems at different pulse repetition frequencies – this is the equivalent of the difference in sweep deviation and rate between FMCW radars. In both radars, interference is reduced by the difference in relative coherence in their relative domains – the closer the sampling parameters of both radars are together the worse is the cross-correlation and therefore the co-interference.

This can be defined in a simple way with the concept of a matched filter – a matched filter is that whose characteristics exactly match in the modulation domain those of the transmitted signal and can therefore recover the maximum energy from the receive signal.

As is shown in Annex 3, such a characteristic is simply described for an FMCW radar – it is the modulation factor given by the product, m = 2FmTd, so much frequency deviation in a given time. For a deviation of 1000 MHz, then for 2FmTd = 1, then Td = 1/2Fm = 0.5ns, the equivalent of a pulsed radar with the same resolution. For a sweep duration of 1ms, then 2FmTd = 2x 106.

For a radar sweeping 1000 MHz in 40ųs, then 2FmTd = 8 x 104. The integrated interference per cycle is 1/35 of the level seen by its own signals at the same incident power level, 15.5 dB less. This figure assumes that the same absolute coherence applies to both signals in both time and frequency domains – both signals are infinitely stable.

As has been found in practise, reducing the level of coherence, either by randomising sweep start times, or by randomising frequency start, reduces the integrated signal level seen in a victim receiver. It can be seen that FMCW radars are in effect Fourier spread spectrum systems and their ability to reject interference is very good and can be substantially improved using modern digital signal process, providing that the correct architecture and processing protocol is chosen.

The model given above shows that all FMCW radars can be described, in terms of their relative compatibility, in terms of an inherent ability to reject interference non-coherent with their own transmissions. This ability is maintained on a per cycle basis but can be rapidly degraded by the serial combination of samples in a strictly periodic manner.

The discussion above shows that the interference levels experienced by the victim are defined by both the interference power level and the characteristics of the victim and interferer FMCW waveforms.

### 2.2.1 Slow and fast chirp FMCW radar

For FMCW radars, the overall processing gain available is related to the product of the sweep time and the sweep frequency.

In slow chirp FMCW radar systems, chirps are sent with a duration of typically 1ms or more. In some cases, a chirp with positive gradient, followed by one with a negative gradient is transmitted to decouple the range-Doppler relationship. The signal received from this small number of chirps is processed using a windowed 1-D FFT to provide a Raw Targets list. The use of multiple Rx channels allows for target azimuth to be estimated.

Fast-chirp FMCW radars transmit a block of chirps, e.g. 128, which are sent in rapid succession, e.g. 128 x 80us. The chirps are processed using an FFT after windowing using a function such as Hamming. The results are then combined using a second windowed FFT function which allows the accumulation of the energy across the full observation period to provide instantaneous range and target speed information in a 2D matrix. The addition of multiple Rx channels creates a third dimension, so this processing is often referred to as 3D processing.

The use of windowing functions prior to the FFT(s) means that the centre of the measurement bandwidth or the centre of the measurement period is more susceptive to interference than the outer edges of the frequency band or measurement period. For example, interference occurring during the first 1/3 of a block of chirps has approximately 1/7th (-8dB) of the level of interference that occurs in all chirps. Similarly, interference occurring during only the first ½ of a block of chirps has ½ (-3dB) the level of interference occurring throughout the chirps.

## 2.3 DESCRIPTION OF AUTOMOTIVE RADARS

### 2.3.1 General information

Automotive radars, operating in the 76-77 GHz band were first introduced in the early 2000's. By 2009, 200,000 units per year were shipped annually in passenger cars and 15,000 in heavy vehicles [8]. This number was forecast to rise to 400,000 units per year and over 1 million units per year for heavy vehicles by 2015. Currently 5% of all vehicles on the streets in Europe are equipped with at least on radar.

At the time of introduction, the price for automotive radars was high. Due to the technology, the deployment in vehicles was low. With evolution in technology and integrated 76 GHz chipsets becoming available the deployment of systems in vehicles is accelerating.

Automotive radars are used extensively for a range of different functions in the vehicle which fall into two categories:

- “Comfort” features provide a warning to the driver such as the presence of a vehicle in the blind spot;
- “Safety related” features actively control the vehicle, such as Autonomous Emergency braking.

Some common radar features are presented in Table 2 below.

**Table 2: Common radar functions**

| | | | |
|---|---|---|---|
| Front – Forward-Looking | Assisted Cruise Control | 250 m – LRR | Comfort |
| | Emergency Autonomous Braking | 50 m – MRR | Safety related |
| Front Corner sensors side-ways looking | Junction Assist | 40 m – SRR | Safety related – input to braking systems |
| | Collision Detect | 40 m – SRR | Safety related – input to airbag control |
| Rear Corner sensors, 45° to vehicle | Blind Spot Monitoring | 10 m – SRR | Comfort |
| | Lane Change Assist | 100 m – MRR | Comfort |
| | Rear Cross-Traffic | 40 m – SRR | Safety related – input to braking systems |
| | Rear or Side Collision Assist | 40 m – SRR | Safety related – input to braking systems |

- Some manufacturers further use the radar information in proprietary ways as input to autonomous driving features and these would be in addition to the common features listed above;
- The beam pattern of an automotive radar is typically matched to the required field of view of the radar;
- The radars are typically concealed behind the fascia/bumper of the vehicle and often a driver would be unaware of their presence. In some cases, the radar data would be combined with data from a camera.

### 2.3.2 RF parameters of automotive radars

Recommendation ITU-R M. 2057 (column A of Table 1) provides some examples of parameters related to automotive radars. In this report, the parameters given in the following table were used instead, because they are considered a more up-to-date and detailed representative of the current status of automotive radars.

### Table 3: Typical technical parameters of automotive radars

| | Front Long range | Front Mid range | Front-side Mid and short range | Rear-side Mid and short range |
|---|---|---|---|---|
| Max operating range @ 10dBsm target size | 250 m | 160 m | 100 m | 100 m |
| Antenna height above road | 0.2 - 1.0 m | | 0.3 - 1.2 m | |
| Antenna lateral offset from vehicle center | Up to +/-1 m | | | |
| Antenna orientation with respect to driving direction | 0° / 0° | 0° / 0° | 0° / +/-30° | 0° / +/-135° |
| Antenna polarization | Horizontal vertical diagonal | Horizontal vertical | | |
| Tx modulation type | Slow FMCW, Fast FMCW | | | |
| Occupied RF bandwidth (typical) | 100 - 250 MHz | 500 MHz | Mid Range: 500 MHz<br>Short Range: up to 1 GHz | Mid Range: 500 MHz<br>Short Range: up to 1 GHz |
| Tx frequency sweep time (typical) | Slow FMCW: 1-20 ms;<br>Fast FMCW: 20-80 µs | | | |
| Tx antenna feed power (typical) | 10 dBm | | | |
| Tx / Rx antenna max. gain (single element) | 20-25 dBi | 15-20 dBi | 15 dBi | 15 dBi |
| Tx / Rx antenna beamwidth(-3 dB) Azimuth | +/-5° | +/-6° | +/-60° | |
| Tx / Rx antenna beamwidth(-10 dB) Azimuth | +/-7° | +/-8° | +/-70° | |
| Tx / Rx antenna beamwidth (-10 dB) Elevation | up to +/-10° | up to +/-10° | up to +/-10° | |
| Tx / Rx sidelobe level relative to peak (dBr) | Normally no Bumper in Front: -25dBr | - 20 dBr | -15 dBr | |
| Tx / Rx typical antenna diagrams | 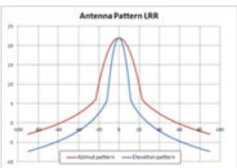  | 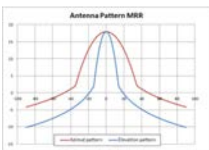  | 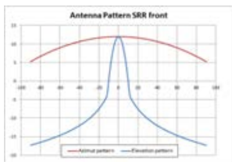  | 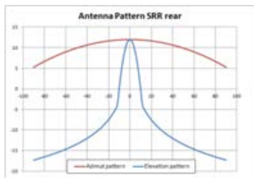  |
| Tx power e.i.r.p. (peak) | 30-40 dBm | 25-30 dBm | 20-25 dBm | 20-25 dBm |
| Tx duty cycle (Ratio of transmit | 20 – 50% | | | |

| | Front Long range | Front Mid range | Front-side Mid and short range | Rear-side Mid and short range |
|---|---|---|---|---|
| on/off ratio) | | | | |
| Rx typical noise figure | 15 dB | | | |
| Rx IF bandwidth (before analog-digital conversion) | Slow FMCW: up to 200 kHz<br>Fast FMCW: up to 15 MHz. | | | |
| Rx IF typical noise floor (before analog-digital conversion) | -99 dBm/MHz<br>N = 10 log10 (kTB) + NF<br>with reference bandwidth B = 1 MHz | | | |
| Rx IF bandwidth (after signal processing) | 500 kHz – 25 MHz | | | |
| Rx-sided typically used interference mitigation | CFAR | | | |
| Rx antenna feed point power for RF 1dB compression | Approx. -10 dBm | | | |
| Rx antenna feed point power for ADC clipping in IF passband | Approx. -40 dBm | | | |
| ADC, typical number of bits | 12 | | | |

For additional details for the above parameters see [12]

### 2.3.3 Spectrum occupation by automotive radars

**Long-range radars** are designed to detect objects at a great distance. Therefore, these systems are using a comparative high Tx-power and are focussing their energy into a very narrow field of view (horizontal angle +/- 5°). As the spatial resolution is of subordinate importance these systems are using only 200-350 MHz of modulation bandwidth.

**Mid-range radars** have a detection range up to 160 m and therefore use less output power then long-range radars. They have azimuth field of view of +/- 6°. Because a more precise spatial resolution is necessary to measure the distances to objects ahead of the vehicle, these systems have an occupied bandwidth up to 500 MHz.

**Short range radars** need to observe the environment in the close vicinity of a vehicle. Therefore, they operate at lower Tx-power-levels, but do have larger fields of view of +/- 60°. These systems usually have a detection range up to 40 m.

As a good range resolution is very important for these systems, and as a good range resolution directly translates into a high occupied bandwidth of up to 1 GHz.

The graphical presentation of these radar types are given in Figure 2.

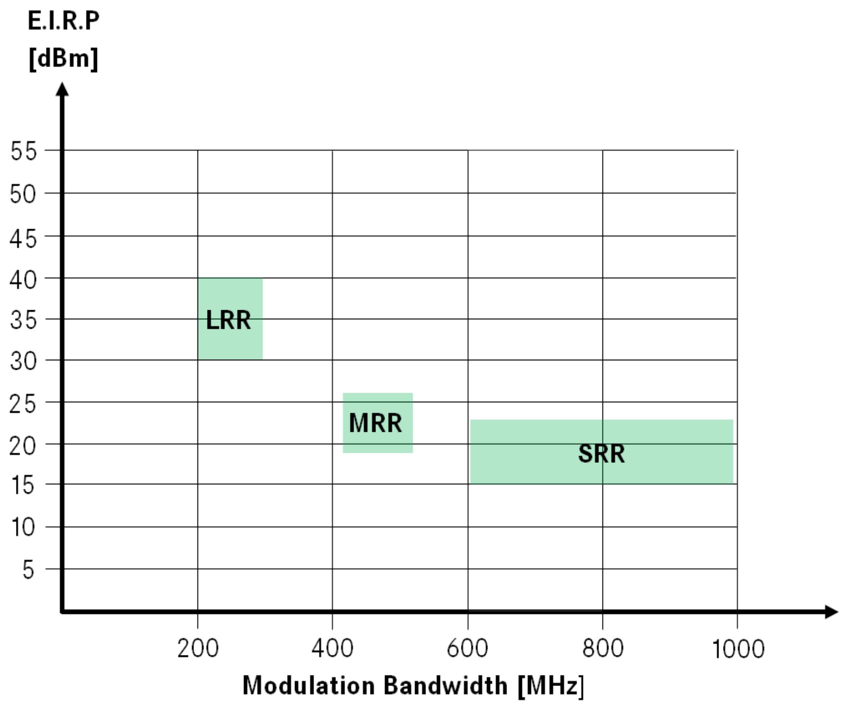


Figure 2: Graphical representation of automotive radars

### 2.3.4 Example of automotive radar deployments

#### *2.3.4.1 Quiet environment*

Currently only 5% of the vehicles on European roads are equipped with one or more radar sensors. This means that only 1 out of 20 cars will have radar sensors on board. Automotive radars are some of the time not exposed to any other radar signals than the reflections of their own intentional signal.

The noise level (N) in this case is coming from thermal noise and unwanted returns of the vehicles' own scattered signal (Clutter). Such unwanted scattered signal returns are coming for example from the road-surface or from various objects at the roadside as can be seen from Figure 3.

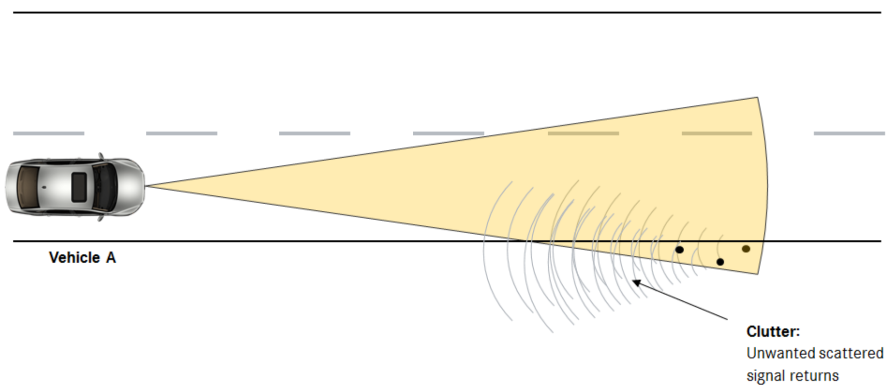


Figure 3: Illustration of unwanted scattered signal returns (Clutter)

### *2.3.4.2 Exposure to indirect signals in an automotive environment*

In the presence of other vehicles with radars the victim vehicle may be exposed to unwanted indirect signal returns of its own radar signal and the unwanted returns that come from the reflections of radar signals from other vehicles. These reflections of signals will appear as an unwanted indirect input of energy into the signal processing chain of the victim radar. In some cases, signals from other radar sources will be obstructed by objects (further vehicles without radars) in between the victim vehicle and the second automotive radar source (see Figure 4).

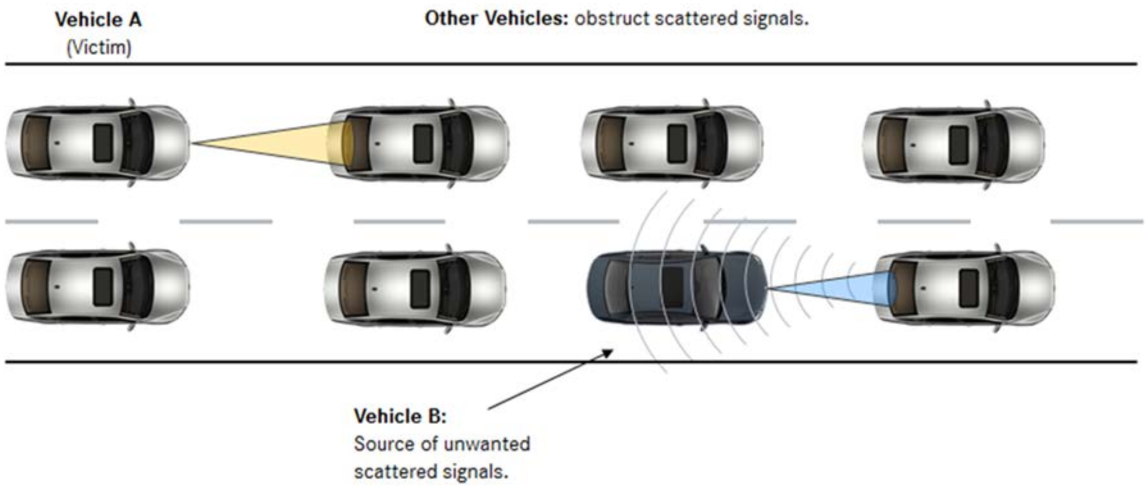


**Figure 4: Illustration of unwanted indirect signals from other automotive radars**

Usually these unwanted indirect signal returns transmit a very low energy that contributes to the noise floor. In some cases, these indirect reflections from foreign radars can be of the same order of magnitude as the return signal of the victim vehicle's own radar. One example of indirect energy input into the victim vehicle's antenna occurs when two vehicles (victim and interferer) that both have front facing radars mounted are going along next to each other on a motorway and a third vehicle (target) is some distance ahead of these two (see Figure 5). Other cases of indirect reflections may occur in other automotive radar installation situations.

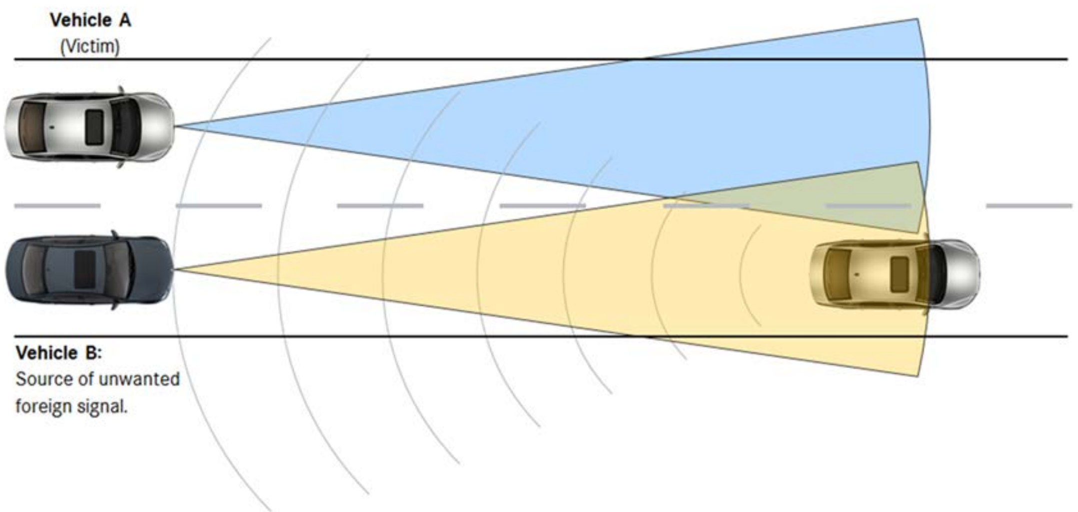


**Figure 5: Illustration of unwanted indirect signals from other automotive radars**

### 2.3.4.3 Exposure to direct signals in an automotive environment

A direct input of unwanted energy into the victim vehicle's antenna can occur when the victim vehicle is illuminated by another vehicle radar. In the example below both vehicles have front facing radars illuminating each other (see Figure 6).

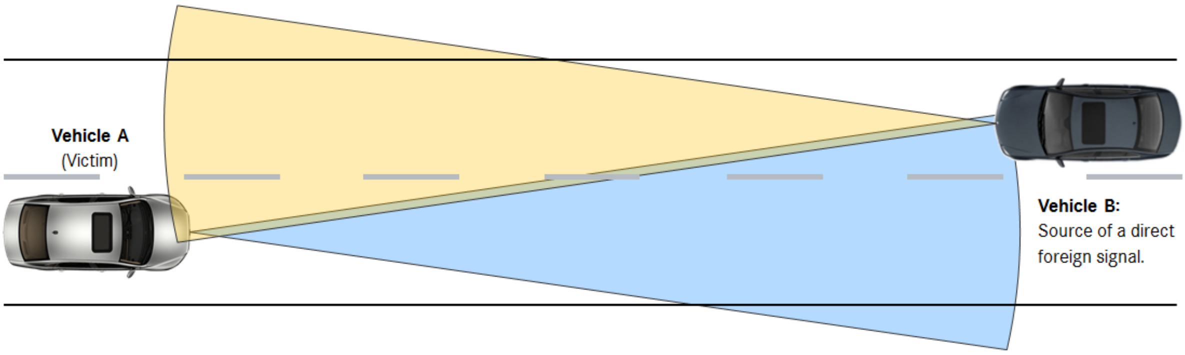


**Figure 6: Illustration of a direct signal from one other automotive radar**

A situation, such as shown in figure 6 can occur on the roads where adjacent lanes have traffic travelling in opposite directions. The duration of such events are dependent on vehicle's speed and may only last for a few seconds until the vehicles have passed each other by and have left the field of view of the other vehicle.

On motorways lane separation is usually greater and there may be guardrails that obstruct radar signals from oncoming traffic. On this type of roads, direct link between two front facing automotive radars may not be so common, but direct links may occur through combinations of front, rear or side looking radars. In these cases, the two vehicles may be driving alongside for some time.

### 2.3.4.4 Interference mitigation

An energy input into the receiver antennas may have negative effects on these systems but it will not necessarily lead to interference. Interference can only occur when the victim radar and the interferer are in the field of view of each other (geometrical orientation) and when their signals overlap in frequency and time. Interference will only occur if all of these conditions are met. These situations are realistic and can occur in practice. Automotive radars have features implemented to mitigate these effects or in the worst case to detect interference and to safely shut down the system.

Some system features that aid mitigation are provided below:

**i. Cycle time**: Cycle time of automotive radar systems usually have a total duration of 40 – 60 ms that can be broken down into a detection period and processing time. The detection periods usually only last 6 – 20 ms (see figure 7). For long range radar systems, the occupied bandwidth typically is 200 - 350 MHz with a detection period of only about 10 ms. Representative values for the various other radar systems are given in Table 4.

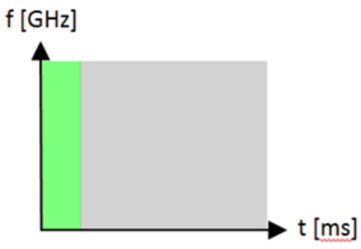


**Figure 7: Representation of an automotive cycle time with its frequency and time domain**

The detection period is represented by the green segment. The grey segment represents processing time.

**Table 4: Typical transmit/receive and compute timing of automotive radars**

| Cycle N | | Cycle N+1 | | Etc. |
|---|---|---|---|---|
| Approx. 6-20 ms | Approx. 30-40 ms | Approx. 6-20 ms | Approx. 30-40 ms | |
| Transmit one or more slow FMCW chirp or many fast FMCW chirps | Signal processing, (RF transmitter powered off) | Transmit one or more slow FMCW chirp or many fast FMCW chirps | Signal processing (RF transmitter powered off) | |
| Digitize analogue signal from all Rx channels | | Digitize analogue signal from all Rx channels | | |

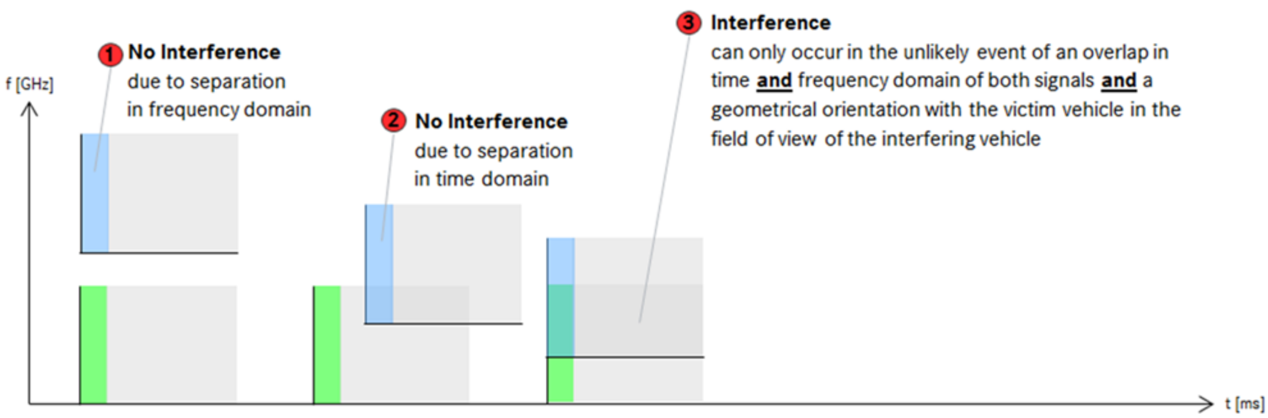


**Figure 8: Interference mitigation by means of cycle time**

Figure 8 displays a representation of two automotive duty cycles. The green segment represents the active (detection) period of the victim vehicle. The blue segment represents the active period (detection period) of the interfering vehicle.

Interference cannot occur if the active periods of the duty cycles of the victim and the interfering vehicle are synchronized in time but do not overlap in frequency domain (see No. 1).

Likewise, interference will not occur if the active periods of the two duty cycles do overlap in the frequency domain but are not synchronised in time (see No. 2). The ratio of the temporal extension of the active periods of the two radar systems related to the passive periods of these two systems determines the probability of interference if these two systems share the same sub-band.

Situation No. 3 shows the situation that the active periods of the two duty cycles do overlap in frequency and time at the same moment. This is the only situation when interference will occur.

## 2.4 DESCRIPTION OF RADAR EQUIPMENT USED FOR FIXED TRANSPORT INFRASTRUCTURE

### 2.4.1 General information

Fixed Radar systems operating in the 76-77 GHz range have the capacity of remotely sensing the environment and detecting moving objects with a high spatial resolution, while affording an antenna of relatively small size compared to other lower bands. This feature makes them a system well suited for Automatic Incident Detection especially for use on motorways and other strategic roads, bridges and tunnels. By continually measuring and tracking vehicles, people and debris using high frequency radar the system is able to generate incident alerts, whilst maintaining extremely low nuisance alarm rates.

The following is a non-exhaustive list of applications, related to transport safety and monitoring:

1 Surveillance radar for traffic incident detection and prevention: Wide area surveillance of roads, to detect events that are highly likely to lead to incidents, is a valuable way of improving the safety of European road networks. These might include early detection of stopped vehicles, reversing vehicles, personnel or animals on a road carriageway, debris on a carriageway due to a lost load.

2 Surveillance radar for traffic enforcement and safety: Enforcing unsafe behaviour of vehicles, unsafe close following of the vehicle ahead, unsafe overtaking or crossing of the central white lines, illegal behaviour at yellow box junctions leading to congestion as busy intersection become congested, enforcing and thereby discouraging dangerous driving manoeuvres such as illegal U-Turns, enforcement where dangerous driving behaviour can lead to loss of life around intersections with other modes of transport, for example, at railway crossings.

3 Road-Railway Crossings (Railway network based): Railway based radars function as obstacle detectors for use only when the crossing is operated as a railway. Generally, they are fixed rather than scanning beam and oriented so as to illuminate the crossing area and the railway track. These would fall under Annex 4 of ERC/REC 70-03 [4]. ETSI introduced a respective harmonised standard ETSI EN 301 091-3 v1.1.1 [9] to cover this application. This standard includes also essential installation requirements and operation requirements.

Other applications, not related to the transport infrastructure are also foreseen, but they are not covered in this report

### 2.4.2 Technical parameters

The main parameters of the scanning fixed transport infrastructure radar considered for this study are given in Table 5.

**Table 5: Technical parameters of the scanning fixed transport infrastructure radar considered for this study**

| Parameter | Value |
|---|---|
| Frequency Range | 76.2 to 76.8 GHz |
| Range of Sensor | 500 m |
| Field of View coverage | 360° full coverage (for scanning systems) |
| Peak Power | 37-40 dBm |
| Average e.i.r.p. in a given direction while rotating | 38dBm+10log(1.8°/360°) = 15 dBm<br>(Section 7.2.3.2. of ETSI EN 301 091-1 V1.3.3 [9]) |
| Sidelobe level in typical deployment | TBD |
| Occupied RF Bandwidth | 650 MHz |
| Rotation speed | Nominal 4Hz rotation rate through 360° taking 400 measurements per rotation. |
| Period of chirp | 625µs |
| Beamwidth in azimuth | 1.8 degrees |
| Main lobe duty cycle (Note) | 0.5 % |
| Mounting Height | Typically, 3-5 m above ground level |
| Distance from side of carriageway | TBC |
| Deployment of infrastructure radar | Typical separation is 350 m to 700 m |

Note: Here the duty cycle is defined as the ratio between the total angle scanned and the azimuth beamwidth of the antenna.

The parameters given in Table 3 are typical values, and depending on the installation scenario they might vary (for instance mounting heights and coverage range). These roadside infrastructure radars have a narrow azimuth beamwidth of 1.8° with a spread elevation beam pattern, (Cosec2) profile allowing more power to be directed at longer ranges, minimising power close in to the radar site.

The infrastructure radar beam boresight is directed at the road surface at a typical distance of approx. 300m

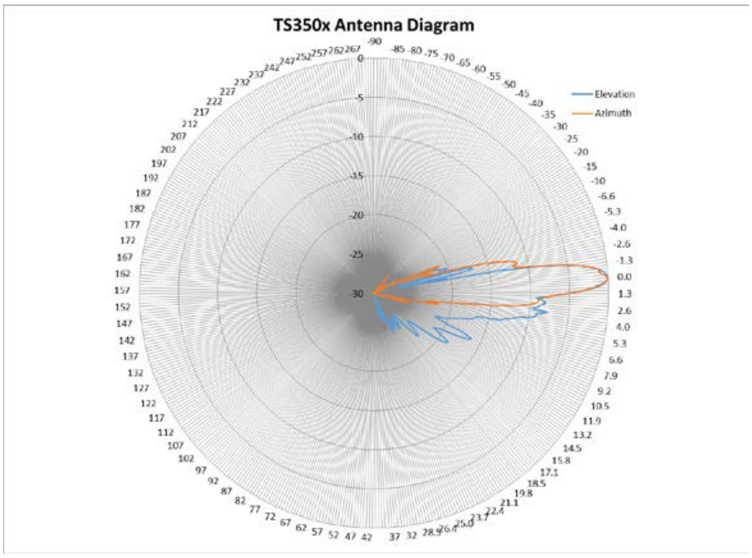


Figure 9: Infrastructure radar elevation and azimuth antenna beam plots in free space

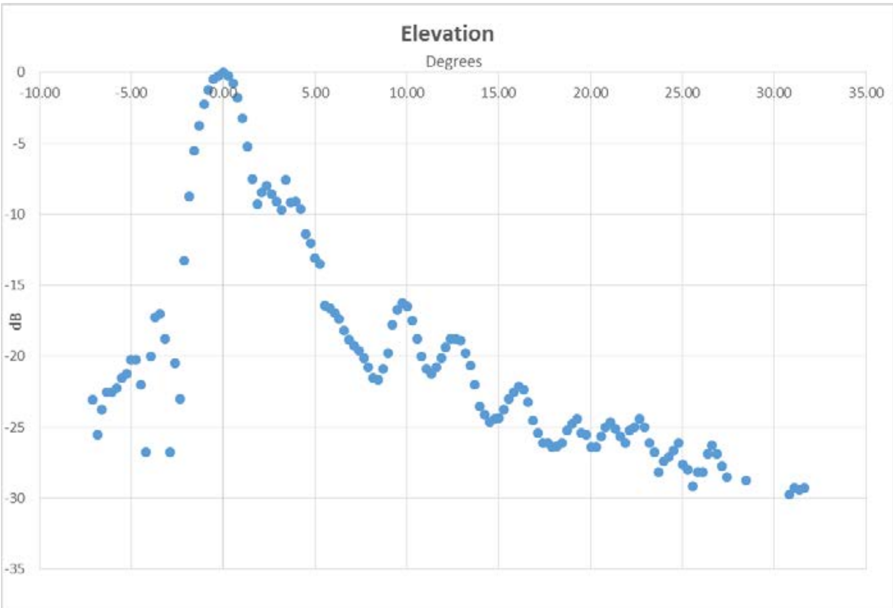


Figure 10: Infrastructure radar elevation and azimuth antenna beam plots in free space

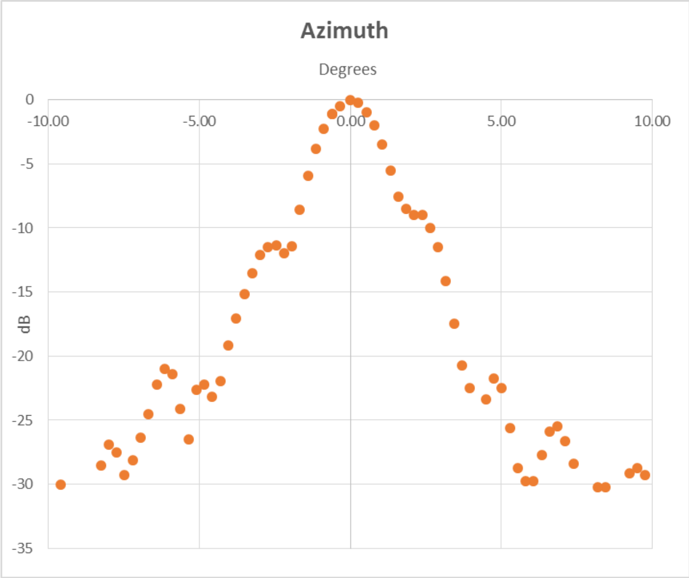


**Figure 11: Infrastructure radar elevation and azimuth antenna beam plots in free space**

Unwanted emissions are within the limits specified by ETSI EN 301 091-1 [9], which is aligned with ERC/REC 74-01 [7].

**DC and Scanning**: It is only necessary to illuminate a given target area intermittently, and at a very low duty cycle. One method of achieving this is with a mechanically scanned antenna. The radar boresight scans a horizontal plane parallel to the road surface. The actual duty cycle depends on the antenna beamwidth in azimuth and is typically 1 in 200. The scan rate normally selected in this system is 4 times per second.

**Rx**: The infrastructure radar includes a single antenna for transmit and receive channels. The radar receiver includes an active mixer that converts the Radio Frequency signal into an Intermediate Frequency or Video range which covers 50 kHz to 5 MHz. The receiver Noise Figure is typically 10 dB at 1 MHz.

**Example of fixed radar deployment scenarios**

Fixed radars are typically deployed along sections of Smart motorways and road tunnels for the applications listed in section 2.3.1.

Installation positions vary between specific radar sites based on application, environmental factors such as highway topography in terms of inclination of road surface and general line of sight issues. The recommended mounting height for the fixed radar considered in this report is 5m. This height usually allows optimum performance for total coverage per radar and reduces obstructions from high sided vehicles that may result in temporary blind spots/azimuths. A study of radar installation sites shows the common mounting is between 4.5-5.5 m above the road surface. No mounting heights above 10m are recorded to date and none expected in the future.

In tunnel applications there can be placement restrictions due to bore height and infrastructure, which can result in mounting heights between 3-5.5 m. These are rare situations and at time of writing only two deployment projects have radars below 4m. It has been seen in some installation projects that radars may be staggered either side of the road.

Figure 12 illustrates an example installation along a section of UK Highway with the radars located at ranges most appropriate for the section of road, in this case approximately 700 m.

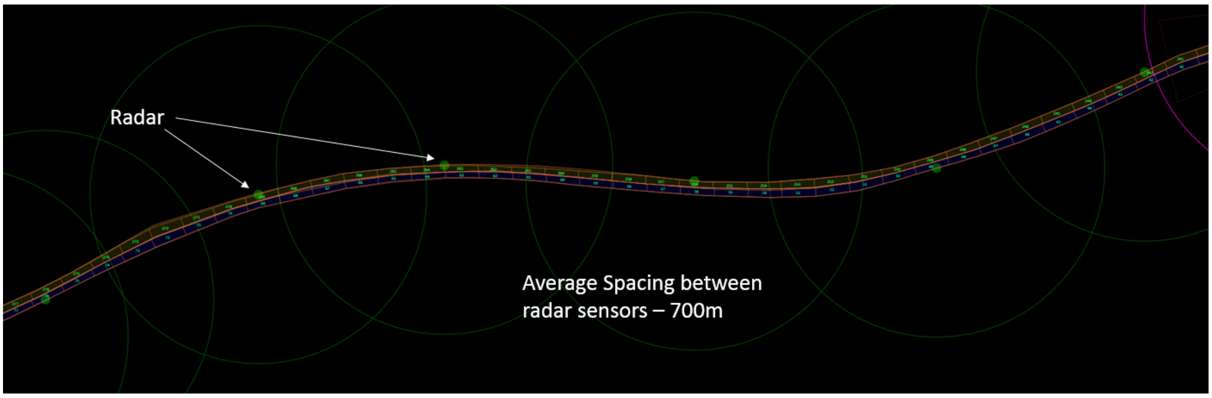


**Figure 12: Typical Fixed Infrastructure Installation on a section of Smart Motorway**

Figure 13 illustrates an example installation site of a fixed transport infrastructure radar.

**Figure 13: Example Fixed Radar Installation Location**

### 2.4.3 Summary

The FMCW radar types considered in this report are summarised for modulation bandwidth, duty cycle and e.i.r.p. in Table 3.

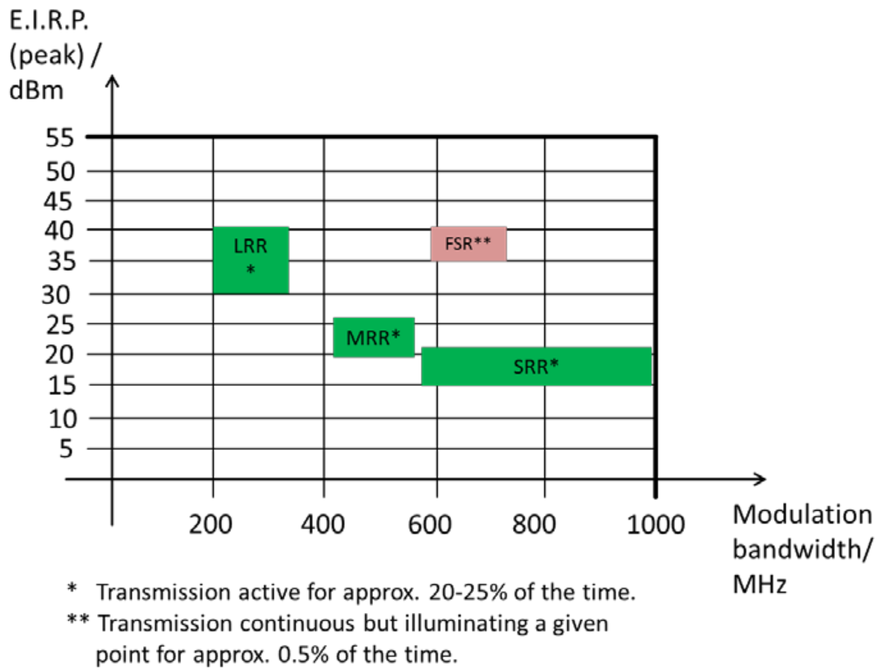


**Figure 14: Overview of used bandwidth and e.i.r.p. for several automotive radars and for fixed radars**

In the following chapters it is investigated how these systems can share the spectrum in typical road scenarios.

# 3 SCENARIOS USED IN THE STUDY

## 3.1 INTRODUCTION

In this section a series of scenarios investigate the energy input into the automotive radar system from a single fixed radar site. In the following scenarios the fixed infrastructure radar is described as the interferer and the primary vehicle is described as the victim.

The signal level received at a victim automotive radar's receive antenna port is related to the geographical positions of the victim and the Interferer, as well as the antenna patterns and the interferer's power level. By varying the installation height of the fixed radar site and its distance to the drive path of the victim vehicle this section investigates the influence of these two parameters on the energy input into the automotive victim receiver antenna.

The Scenarios comprise of a typical automotive radar installed in a vehicle, with both a fixed radar and a second automotive radar as interferers. This section describes the selected scenarios and geometries that are considered in this report.

In this study, automotive radar system C is considered. Lorries and trucks are excluded from this consideration

The scenarios, as far as possible, include a main beam to main beam interaction between the vehicle radar and a fixed radar, so as to capture the worst case situation. As the vehicle moves past and the fixed radar antenna rotates, the effect of side lobe coupling can also be observed. In section 5, an MCL calculation is performed to estimate the signal energy incident into the vehicle radar receiver antenna.

Equally important is to establish a reference level and in order to do this a reference transmitter, in the form of a second radar equipped vehicle is introduced. The purpose of including a second automotive radar is to allow the signal level from the fixed radar to be compared to the signal level of a second automotive radar (reference Interferer). The intention is to include, as far as possible, a main beam to main beam interaction between the two vehicle radars. The purpose is not to study the vehicle to vehicle interference.

## 3.2 SCENARIOS

### 3.2.1 Reference Case

The geometry of the setup for the reference case is similar to the test setup of the field test in Neuhausen.

#### *3.2.1.1 Geometrical setup for the Reference Case*

Figure 15 displays the setup of the reference case for the simulations.

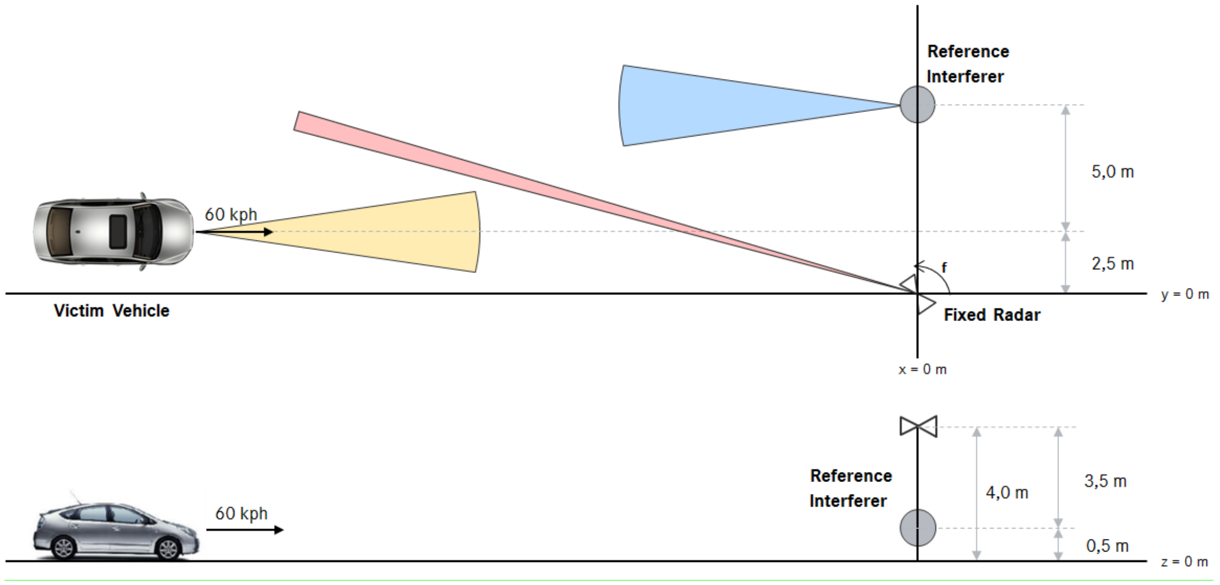


Figure 15: Geometrical setup for the reference case for the simulations

### *3.2.1.2 Parameters of the Fixed Radar Site for the reference case*

The fixed radar is located at the centre of the coordinate system at x = 0 and y = 0 m. The fixed radar is mounted at a height of z = 4 m. According to the values given in this report the fixed radar parameters are set according to Table 6.

Table 6: Parameters for the fixed radar site in the reference case

| Fixed radar (Tx) | |
|---|---|
| Position x (m) (do not change value) | 0 |
| Position y (m) (do not change value) | 0 |
| Position z (m) =mounting height | 4 |
| Main beam el. tilt (deg) (pos=down) | 0 |
| Rotation angle alpha at t=0s (deg) | 0 |
| Rotation speed (deg/s) (pos or neg) | 1440 |
| Tx feed power (dBm) | 10 |
| Tx max. antenna gain (dBi) | 28 |
| Sidelobe floor, relative to main beam (dBr) | -25 |

### *3.2.1.3 Parameters of the Victim Automotive Radar*

The technical parameters of the automotive radar system C according to the field test in Neuhausen were chosen to represent the automotive victim radar. Table 7 displays the parameters for this radar.

**Table 7: Technical Parameters of the victim automotive radar**

| Victim radar (Rx) | | |
|---|---|---|
| Antenna x (m), posn at t=0 | | -200 |
| Antenna posn y (m) | | 2,5 |
| Antenna posn z (m) | | 0,5 |
| Speed (km/h) x axis | | 60 |
| Main beam relative to vehicle driving dir. (beta1 / deg) | | 0 |
| Rx max. antenna gain (dBi) | | 25 |
| Antenna elevation -3dB beamwidth (deg) | | 24 |
| Antenna Azimuth -3dB beamwidth (deg) | | 4,8 |
| Sidelobe floor, relative to main beam (dBr) | | -20 |
| Rearlobe floor, relative to main beam (dBr) | | -50 |

### *3.2.1.4 Parameters of the Vehicle*

The vehicle is positioned at x = -200 m and y = 2.5 m. It has a constant speed of 60 kph and is driving in a direct line towards the fixed radar site.

### *3.2.1.5 Parameters of the Reference Interferer*

The technical parameters of the automotive radar system C according to the field test in Neuhausen were chosen to represent the reference interferer. Table 7 displays the parameters for this radar.

**Table 8: Technical Parameters of the reference interferer**

| Reference Interferer (Tx) | | |
|---|---|---|
| Antenna x (m), posn at t=0 | | 0 |
| Antenna posn y (m) | | 7,5 |
| Antenna posn z (m) | | 0,5 |
| Speed (km/h) x axis | | 0 |
| Tx feed power (dBm) | | 10 |
| Main beam relative to vehicle driving dir. (beta2 / deg) | | 0 |
| Tx max. antenna gain (dBi) | | 20 |
| Antenna Elevation -3dB beamwidth (deg) | | 12 |
| Antenna Azimuth -3dB beamwidth (deg) | | 18 |
| Sidelobe floor relative to main beam (dBr) | | -20 |
| Rearlobe floor relative to main beam (dBr) | | -50 |

### *3.2.1.6 Variation of the Mounting Height of the Fixed Radar*

To consider the influence of the mounting height of the fixed radar on the incident power-level into the victim automotive vehicle radar system the mounting height of the fixed radar was set to z = 3.5, 4.0 and 5.0m.

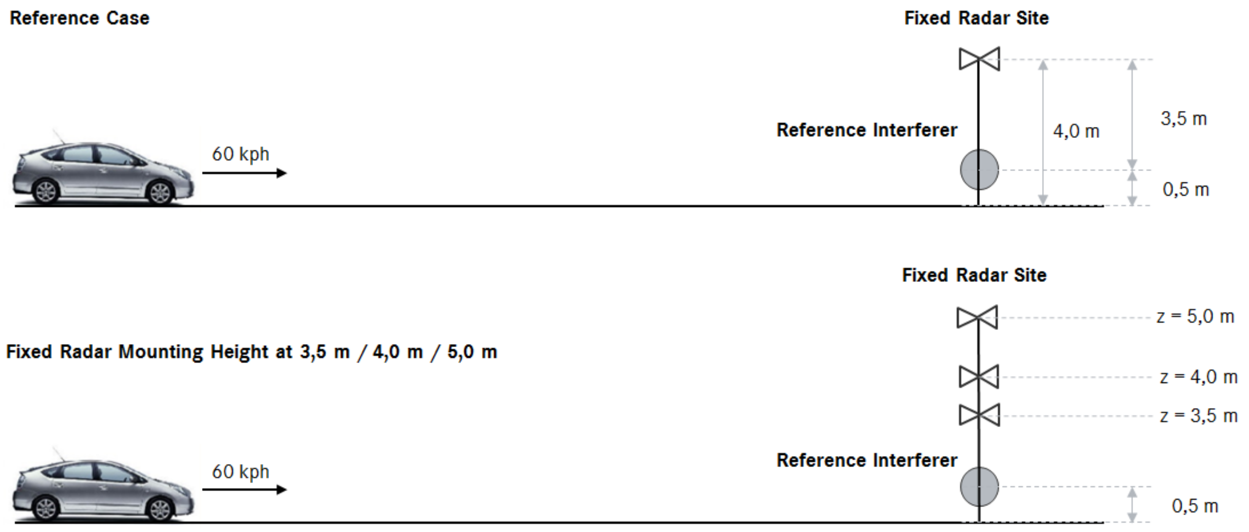


**Figure 16: Variation of the Mounting Height of the Fixed Radar**

### *3.2.1.7 Variation of the Fixed Radar's Distance to the Victim's traffic lane*

To consider the influence of the horizontal distance between the fixed radar site and the traffic lane of the victim vehicle, the distance of the alternative fixed radar position was set to y = -5 m (instead of y = 0 m). Thus the total distance between the fixed radar's y-position and the central axis of the victim vehicle is 7.5 m in this scenario.

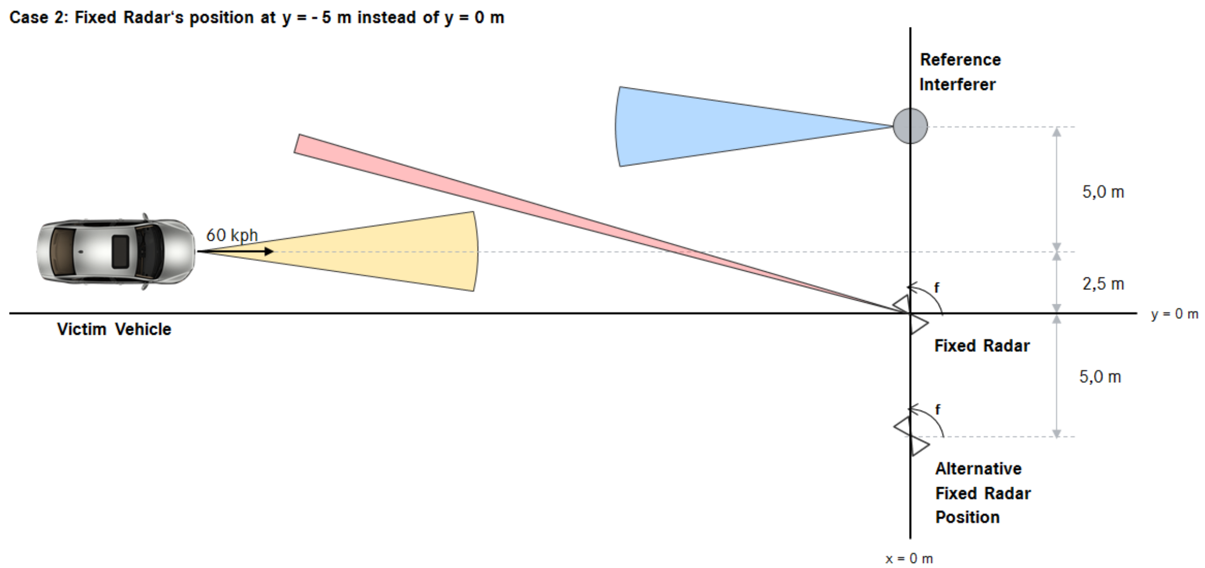


**Figure 17: Variation of the Fixed Radar's Distance to the Victim's traffic lane**

### 3.2.2 Secondary roads Scenario

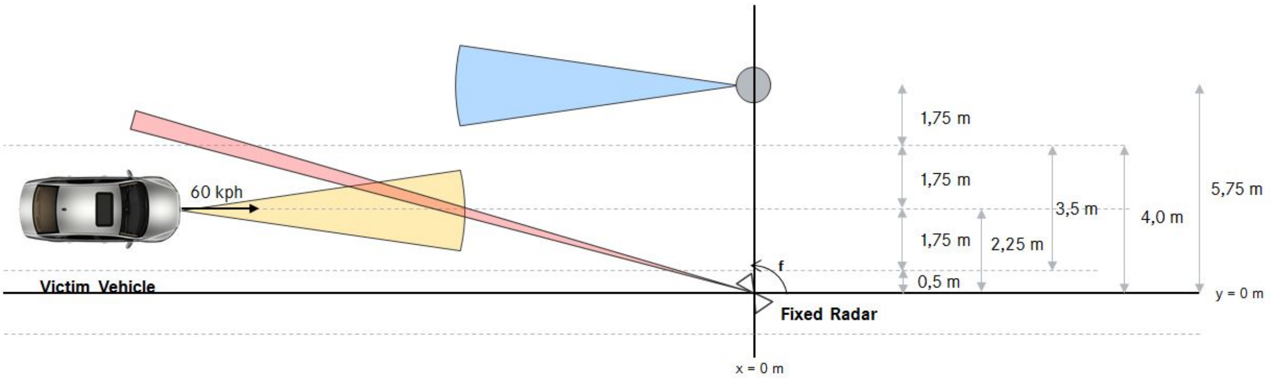


Figure 18: Secondary roads scenario

#### 3.2.2.1 Geometrical Setup of the secondary road scenarios

This set of scenarios illustrates main beam to main beam interaction between a fixed radar and the automotive victim radar as well as between the victim vehicle and the reference interferer vehicle in the adjacent lane. The lane width has been chosen to represent a typical value for secondary roads. The scenario compares the incident power from a typical fixed radar studied in this report into the receive antenna of the automotive system C studied in this simulation.

In these scenarios the vehicle is positioned at x = -200 m and y = 2,5 m. It has a constant speed of 60 kph and is driving in a direct line towards the fixed radar site.

#### 3.2.2.2 Parameters of the fixed radar

The parameters for the fixed radar in this scenario are given in the Table 9 below. Unlike than in the reference case the mounting height of the fixed radar has been set to 5 m, which represents a more typical mounting height than 4 m.

Table 9: Parameters for the fixed radar

| Fixed radar (Tx) | |
|---|---|
| Position x (m) (do not change value) | 0 |
| Position y (m) (do not change value) | 0 |
| Position z (m) =mounting height | 5 |
| Main beam el. tilt (deg) (pos=down) | 0 |
| Rotation angle alpha at t=0s (deg) | 0 |
| Rotation speed (deg/s) (pos or neg) | 1440 |
| Tx feed power (dBm) | 10 |
| Tx max. antenna gain (dBi) | 28 |
| Sidelobe floor, relative to main beam (dBr) | -25 |

### 3.2.2.3 Parameters of the victim automotive Radar – System C

**Table 10: Parameters of the victim automotive Radar – System C**

| Victim radar (Rx) | | |
|---|---|---|
| Antenna x (m), posn at t=0 | | -200 |
| Antenna posn y (m) | | 2,25 |
| Antenna posn z (m) | | 0,5 |
| Speed (km/h) x axis | | 60 |
| Main beam relative to vehicle driving dir. (beta1 / deg) | | 0 |
| Rx max. antenna gain (dBi) | | 25 |
| Antenna elevation -3dB beamwidth (deg) | | 24 |
| Antenna Azimuth -3dB beamwidth (deg) | | 4,8 |
| Sidelobe floor, relative to main beam (dBr) | | -20 |
| Rearlobe floor, relative to main beam (dBr) | | -50 |

### 3.2.2.4 Parameters of the reference interferer – System C

**Table 11: Parameters of the reference interferer – System C**

| Reference Interferer (Tx) | | |
|---|---|---|
| Antenna x (m), posn at t=0 | | 0 |
| Antenna posn y (m) | | 5,75 |
| Antenna posn z (m) | | 0,5 |
| Speed (km/h) x axis | | 0 |
| Tx feed power (dBm) | | 10 |
| Main beam relative to vehicle driving dir. (beta2 / deg) | | 0 |
| Tx max. antenna gain (dBi) | | 20 |
| Antenna Elevation -3dB beamwidth (deg) | | 12 |
| Antenna Azimuth -3dB beamwidth (deg) | | 18 |
| Sidelobe floor relative to main beam (dBr) | | -20 |
| Rearlobe floor relative to main beam (dBr) | | -50 |

# 4 MCL ANALYSIS

## 4.1 INTRODUCTION

A simulation tool has been developed to calculate the incident power received by an automotive radar from several sources. The sources in question are a single fixed transport infrastructure radar site and a reference interferer in the form of a second radar equipped vehicle. The purpose of including a second automotive radar is to allow the signal level from the fixed radar to be compared to the signal level of a second automotive radar (reference Interferer). The purpose is not to study the vehicle to vehicle interference.

## 4.2 SPACE AND TIME SIMULATION TOOL

To represent a vehicular radar, the simulation tool uses the physical principles that are described by Annex 1. It calculates the incident power as received by the automotive victim radar system at the receive antenna. The victim vehicle travels along a straight road at a given speed and passes a fixed transport infrastructure radar site that is located next to the road.

This setup is just a small snapshot of possible scenarios that can be analysed with the MCL calculator.

The simulation is based on time steps. At each step in the simulation, the power received at the victim radar antenna is calculated based on:

- The relative positions of the devices;
- The antenna pointing directions;
- The antenna patterns in the relevant directions;
- The transmitter powers and time domain characteristics;
- Free space propagation.

For the purposes of comparison, the reference emitter is show as stationary in the setup.  This is done so that the effect of both transmitters is shown relative to the same fixed position with just the victim vehicle moving. This simulator scenario does not assume that a vehicle would necessarily be transmitting whilst stationary.

The main purpose of the simulator is to explore the incident power of unwanted signals experienced by the radar receive antenna in several scenarios.

The simulation tool only calculates incident power levels at the victim’s receiver antenna. Incident power alone does not directly transfer into interference. Incident power is only one aspect of interference being generated in the receiver. The simulation tool does not consider any system level or mitigation aspects beyond the receive antenna such as e.g. occupied bandwidth, frequency hopping, duty cycling.

Known limitations and simplifications are:

- Polarisations are assumed to be matched. In practice polarisation mismatch will reduce the signal levels.
- Single ray propagation is assumed; i.e., no multipath from road or any vertical surfaces such as tunnel walls or guardrails. In practice reflections may occur which could either increase or decrease the effects simulated in this tool.
- A flat sidelobe level is assumed outside the region where main beam data is available.
- The automotive antenna patterns use a highly simplified model which means that the results would not completely match reality.
- Antenna data is not available for all elevation and azimuth directions. The simulator works with separate antenna and elevation patterns and assumes that the 2D pattern can be created by adding the dB values in the two axes.

- The simulator makes far-field assumptions for all path-loss calculations. Therefore some small errors may be introduced at short ranges due to antenna near field effects.
- Perfect alignment has been assumed. Manufacturing, assembly, loading tolerances may lead variations
- The fixed infrastructure radar and automotive radar systems studied in this work Item report all differ in their occupied bandwidth use and centre frequencies. In practice these systems may be operating mitigation techniques in relation to occupied bandwidth on a cycle to cycle basis and indeed may be operating in different parts of the band at any given point in time. The simulation does not take this into account.
- As the simulator is currently setup, it does not present incident power received by the victim fixed radar from the interfering automotive radar, therefore these situations have not been analysed. The simulator can be modified to allow this analysis to take place

At present the Time and Space Simulation Tool is still under development. Particularly the implementation of worst-case sidelobe levels is still a matter of discussion.

**Results of the Simulations**

It is important to note a key difference between the Neuhausen test results and the MCL-Results. The results presented from the Neuhausen field trials represented recorded interference power-levels, whereas the simulator results only consider incident power-levels on the receiver antenna.

**Reference case**

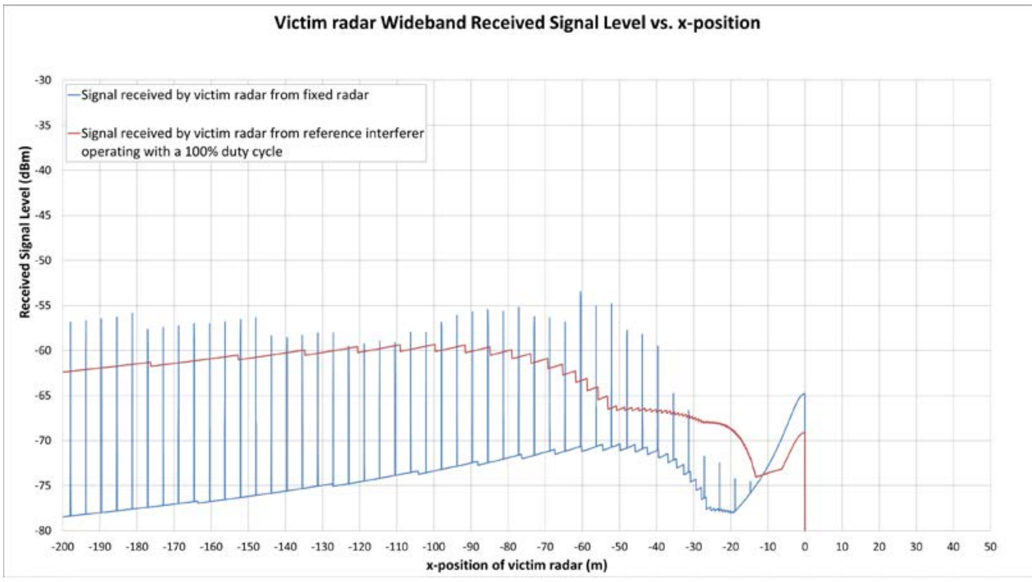


**Figure 19: Energy input into the victim vehicle's receiver antenna from the fixed radar site according to the parameter settings of the reference case**

### Variation of the Mounting Height of the Fixed Radar

In this scenario the fixed radar is mounted at a height of z = 3.5 m, z = 4.0 m and z = 5 m.

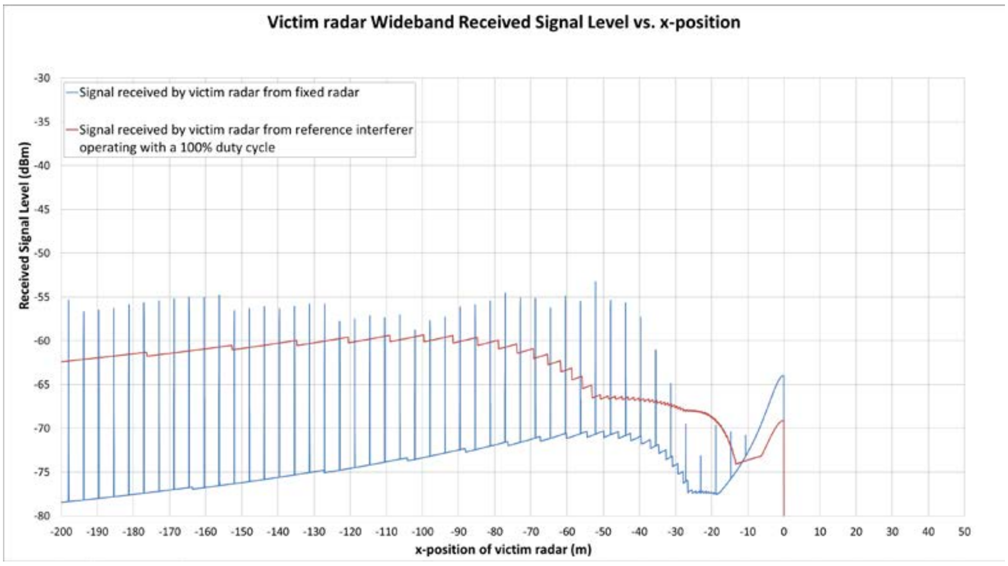


**Figure 20: Energy input into the victim vehicle's receiver antenna from the fixed radar site. Mounting height of the fixed radar set to z = 3.5 m**

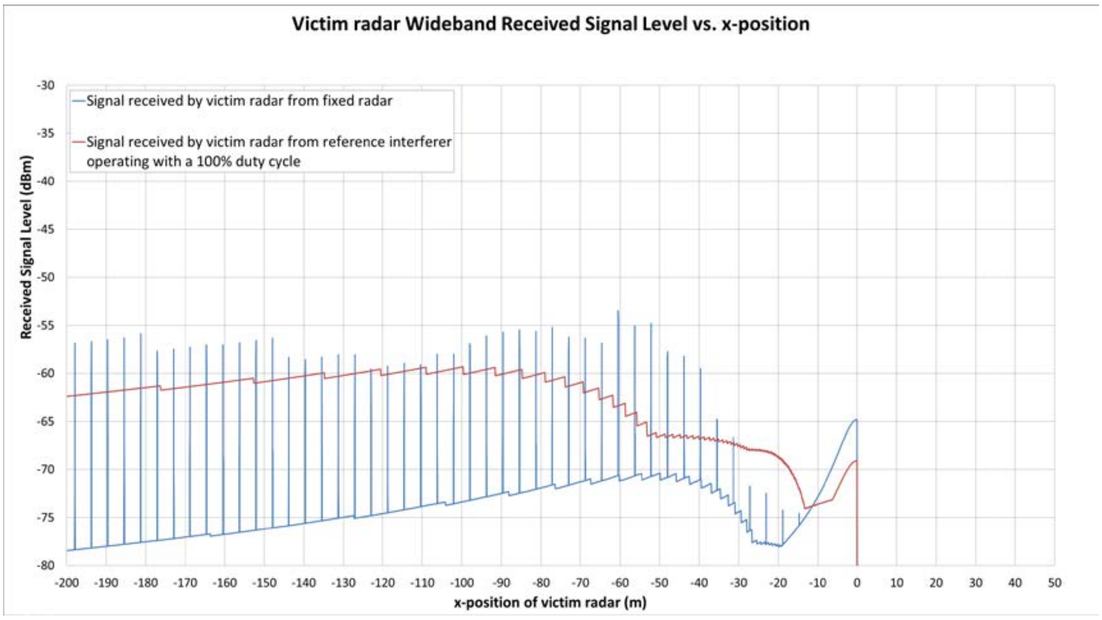


**Figure 21: Energy input into the victim vehicle's receiver antenna from the fixed radar site. Mounting height of the fixed radar set to z = 4.0 m**

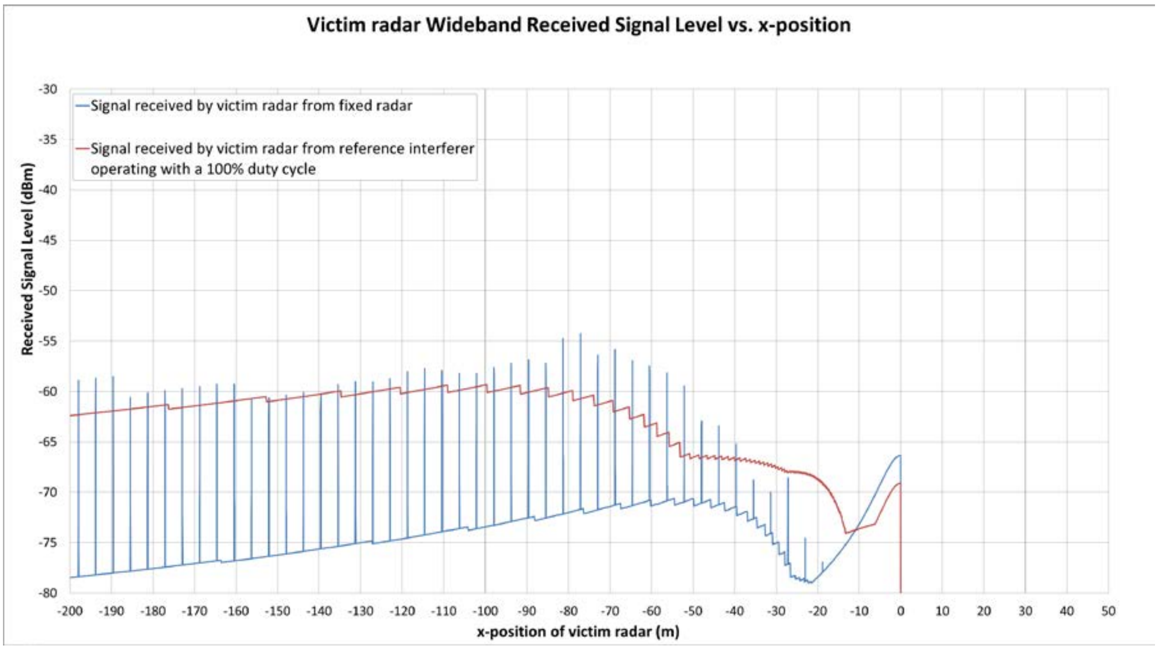


**Figure 22: Energy input into the victim vehicle's receiver antenna from the fixed radar site. Mounting height of the fixed radar set to z = 5.0 m**

Variation of the Fixed Radars Distance to the victim's traffic lane

In this scenario the fixed radar is located at y = -5 m instead of y = 0 m.

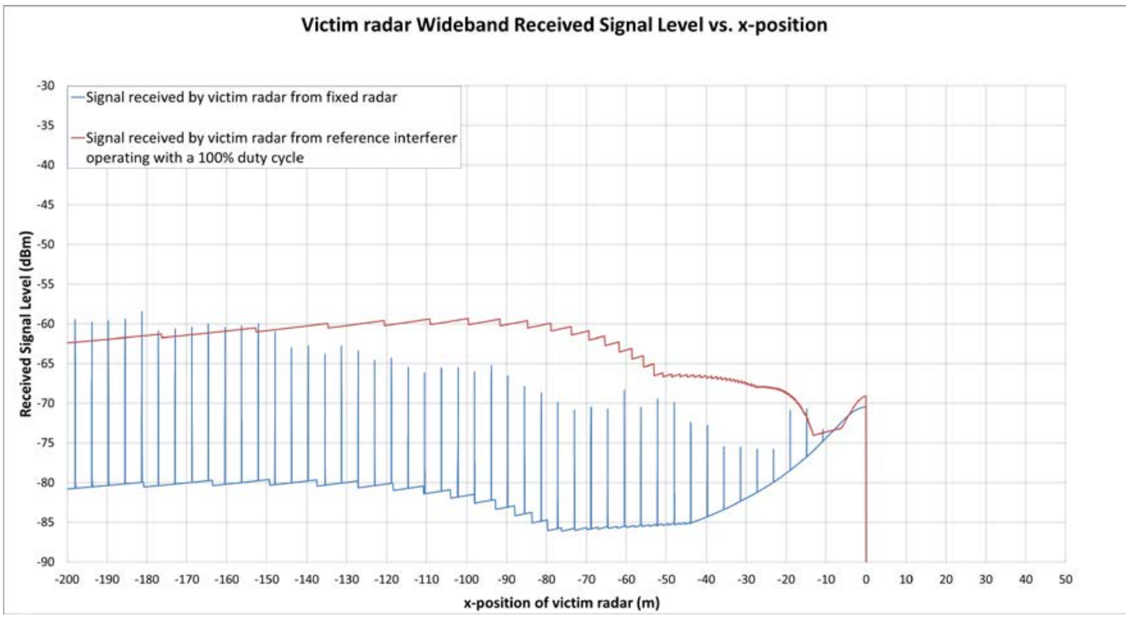


**Figure 23: Energy input into the victim vehicles receiver antenna from the fixed radar site. Mounting position of the fixed radar set to y = - 5 m instead of 0 m**

**Secondary road scenario – system C**

In this scenario the fixed radar is located at y = 0 m.

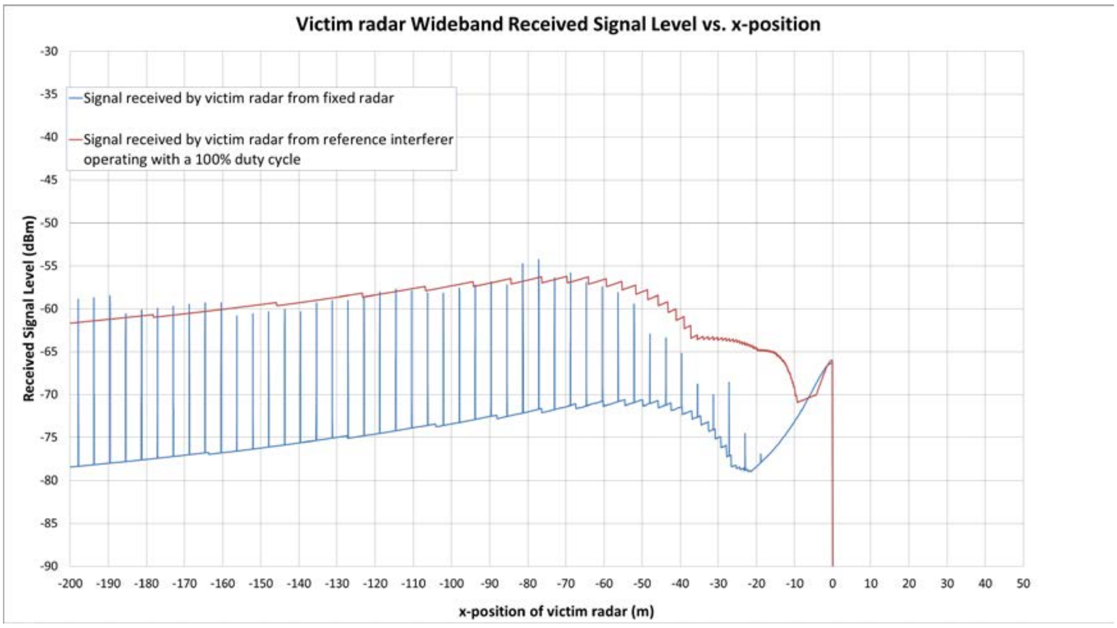


**Figure 24: Energy input into the victim vehicle's receiver antenna from the fixed radar site according to the secondary roads scenario**

## 4.3 INTERPRETATION

The simulations show that the victim vehicle experiences an incident power input from the fixed radar (blue curve) that re-appears when illuminated by the fixed radar with every rotation whilst in the FOV. Whilst the victim vehicle is not illuminated the fixed radar a baseline level of incident power is shown in the results. The baseline display corresponds to sidelobe interaction between the fixed and the automotive antenna systems. A flat sidelobe level is assumed outside the region where main beam data is available. This is one of the known limitations of the simulation tool.

In the scenarios the incident power-level from the reference interferer represents the energy level that could expected from the automotive radar reference emitter described for system C. In the simulations this power level appears as a solid red line because the simulation tool is assuming that the reference interferer is constantly transmitting. A real automotive radar system would send out energy only during the active period of its duty cycle (detection time) which is typically between 20-50% as per Table 3. Therefore, the signal of a real automotive radar would appear as an intermittent signal as well. The simulation is creating a solid line at the peak power limit that could be expected from an automotive radar system in order to facilitate the comparison of this reference energy level to the incident power from the fixed radar

### 4.3.1 Reference case

In the reference case the incident power-level from the reference interferer represents the energy level that could expected from the vehicular radar system C. Figure 28 illustrates that the peak incident power from the fixed radar can be 5 dB above the peak incident power level received from the vehicular radar.

### 4.3.2 Variation of the mounting height

The comparison of the two figures given below (fixed radar mounted at z = 3.5 m, and at z = 5.0 m) shows that the peak incident power input from the fixed radar at 5 m is roughly 1 dB lower than the peak incident power input from the fixed radar at 3.5 m. Incident power-levels at a given range may vary up to 5 dB with the given variation in height. The two figures below show the peak incident power-levels calculated across the full range from these simulations.

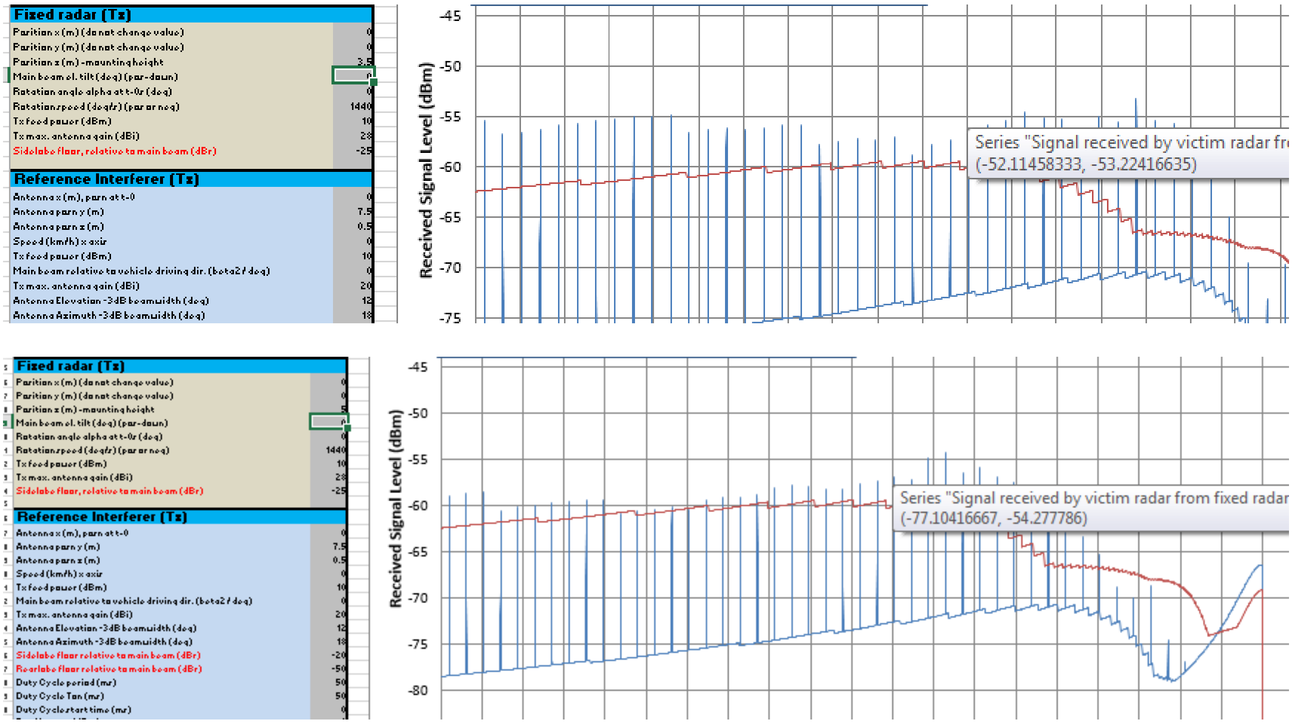


**Figure 25: Peak incident power-levels calculated across the full range**

### 4.3.3 Variation of the Fixed Radars Distance to the victim's traffic lane

The incident power received by the victim automotive radar is significantly reduced due to the larger lateral separation of the fixed radar from the roadside. This effect becomes more obvious and significant as the vehicle approaches the fixed radar site. In the near field it leads to a reduction of the incident power of up to 10 dB. Similarly, the effect will also be reduced for vehicles travelling in lanes 2, 3, etc. in a highway environment.

In Combination the subchapters 4.3.2 and 4.3.3 demonstrate that the incident power level received by the victim automotive receiver depends on the spatial separation between receiver and transmitter. This distance is given be $\sqrt{a^2 + b^2}$ with a being the lateral and b being the horizontal separation of transmitter and receiver. This means that raising the minimum height of fixed radar installations above ground or the lateral distance of fixed radar sites from roadsides could be instruments to reduce the incident power level received by the vehicular radar system.

### 4.3.4 Secondary road scenarios

In this scenario the fixed radar incident power to the victim radar (System C) is analysed. The setup for this scenario has the victim vehicle and the reference emitter vehicle travelling in opposite directions in adjacent lanes. This differs from Neuhausen reference case where the lateral separation from the reference vehicle is greater.

In this particular geometric setup the incident power from the fixed radar and the reference emitter have similar peak levels over the full driving distance, except for very close to the fixed radar where the vehicle temporarily drops out of the field of view of the radar.

**Summary of scenario analysis**

Only a small snapshot of possible geometric scenarios was selected for presentation in this report. Other geometries are possible and the other radar systems studied in this report are not analysed in this section. The simulator has not been used to analyse the incident power received by the victim fixed infrastructure radar from an interfering automotive radar in this report, but could be modified to do so.

Changes to incident power into the victim vehicle can increase or decrease with relative geometrical variations of the fixed radar or another automotive radar (reference emitter in this study).

The incident power received by the victim automotive radar from a fixed radar site, as studied in this report, at its receive antenna can be of the same order of magnitude as the power received from a second automotive radar.

The simulation tool only calculates incident power levels at the victim's receiver antenna. Incident power alone does not directly transfer into interference. Incident power is only one aspect of interference being generated in the receiver. The simulation tool does not consider any system level or mitigation aspects beyond the receive antenna such as e.g. occupied bandwidth, frequency hopping, duty cycling.

The transmit power levels considered in these simulations are realistic values taken for both the fixed infrastructure radar and automotive radars. Radar systems of any type that use more transmit power may have effects stronger than those illustrated in this report.

# 5 SEAMCAT SIMULATIONS

Because of the following reasons no SEAMCAT scenario was considered in this report.

In this report, the operation of automotive radars is explained which indicates that snapshot images of the environment are generated within the radar each cycle and that these raw targets are observed over several successive cycles in order to create tracked targets. Input from the radar to the customer or vehicle is only provided based on the position and speeds of these tracked targets.

For this study we have therefore considered the time-domain nature of interference for a victim travelling along a linear path. It was considered that an Excel spreadsheet that calculates signal level was the most effective way of considering this rather than a Monte Carlo simulation

# 6 FIELD TRIAL MEASUREMENTS AND OBSERVATIONS

## 6.1 CONTROLLED FIELD TRIAL MEASUREMENTS IN NEUHAUSEN OB ECK

### 6.1.1 Description of the test setup

#### *6.1.1.1 Test Area*

The controlled field trial measurements were performed on an airfield at Neuhausen ob Eck, Germany. The airfield is a very large compound that is free from any large objects such as trees or buildings that could cause radar reflections. The airfield was also free from other radar interferers. The weather conditions were very good: sunny clear sky, no cloud cover, no snow or rain.


**Figure 26: Display of the runway and the test-setup during the field test**

The test site offered ideal test-conditions for a compatibility study since no harmful influences on the results had to be expected neither due to signal reflections from large buildings or objects nor due to signal impairment due to bad weather. For the interpretation of the test results it has to be taken into account, that these idealised test-conditions do not reflect these aspects of real life environments.

#### *6.1.1.2 Radar systems*

Subject to the compatibility study were two forward looking automotive long range radar systems, one automotive short range radar system and one fixed transportation infrastructure radar system.

The long range radar systems were mounted to the front of the vehicle and facing into the direction of travel. The short rang radar system was mounted to the corners of the rear bumper of a vehicle and were looking backwards at 45°.

**Figure 27: Representation of the mounting positions of a front-looking long range radar system (left) and a rear looking short range radar system (right)**

The fixed radar installation was mounted on a mobile pole at a hight of four meters that was located on the shoulder of the runway.

#### *6.1.1.3 Targets*

During the field test corner reflectors were used as targets for the radar observation. The corner reflectors were choosen to represent the typical reflection of a pedestrian, a motorcycle and a vehicle.

#### *6.1.1.4 Test Program*

During the test the following cases were considered:

- Fixed radar vs automotive radars;
- Automotive radars vs fixed radar;
- Automotive radar vs automotive radar, as a reference case.

The Test programme for the compatibility study on the fixed radar side was designed to comprise of scenarios with the fixed radar in scanning (rotating) and non-scanning (non-rotating) operation. For both of these cases all three operating-modes of the fixed radar device were applied.

Some measurements were performed with the fixed radar non-scanning. This case is not representive for the fixed radar considered in this report, but can give information about possible non-scanning fixed radar applications not considered in this report.

On the side of the automotive radar systems the test programme consisted of dynamic tests where the vehicles would approach the fixed radar site from beyond the 500 m line at a constant speed of 60 kph and stationary scenarios, where the vehicles would be standing motionless at the 80 m line.

The combination of the operational parameters on both sides leads to a test program as displayed by Table 12. This test program was applied on any combination of automotive radar systems and the fixed radar system.

**Table 12: Test Program for any given combination of the fixed radar and anyone of the automotive radar systems**

| Mobile Radar Position (Front, Rear) | Fixed Radar Rotation | | Car Parameters | | Fixed Radar Parameters | | |
|---|---|---|---|---|---|---|---|
| | | | | | Mode | Sweep (ms) | Rotation (Hz) |
| F | 2 | Fixed Radar (without Rotation) | s | stationary car | 1 | 2.000 | 0 |
| | | | | | 2 | 1.250 | 0 |
| | | | | | 4 | 0.625 | 0 |
| | | | d | dynamic car | 1 | 2.000 | 0 |
| | | | | | 2 | 1.250 | 0 |
| | | | | | 4 | 0.625 | 0 |
| | 3 | Fixed Radar (with Rotation) | s | stationary car | 1 | 2.000 | 1 |
| | | | | | 2 | 1.250 | 2 |
| | | | | | 4 | 0.625 | 4 |
| | | | d | dynamic car | 1 | 2.000 | 1 |
| | | | | | 2 | 1.250 | 2 |
| | | | | | 4 | 0.625 | 4 |

Even though vehicle versus vehicle testing is not subject of this study some tests were performed according to the pattern given by Table 13 to provide a reference.

**Table 13: Test Program for vehicle vs vehicle testing**

| Position Radar 1 (Front, Rear) | Position Radar 2 (Front, Rear) | Car Parameters | | Mobile Radar Parameters | |
|---|---|---|---|---|---|
| | | | | Radar 1 | Radar 2 |
| F | F | s | stationary | on | on |
| F | F | s | stationary vs stationary | on | off |
| F | F | | | off | on |
| F | F | d | stationary vs dynamic | on | on |
| F | F | | | off | on |
| F | F | d | stationary vs dynamic | on | on |
| F | F | | | off | on |

### *6.1.1.5 Test Setup*

During the test the fixed radar site (F) was mounted on a mobile pole at a hight of four meters on the right shoulder of the runway. The Targets T1 – T3 were positioned at a distance of 35 m to 50 m from the fixed radars position. T2 was located right on the centre line of the runway, the targets T1 and T3 were position 5m meters above and below that line at a horizontal distance of 5 m.

T4 was set up as a beacon to support the orientation and interpretation of the fixed radars signals. The 500 m line represents roughly the rim of the field of view of the fixed radar site on the runway.

Targets T1 to T4 were mounted at a height of 50 cm above ground.

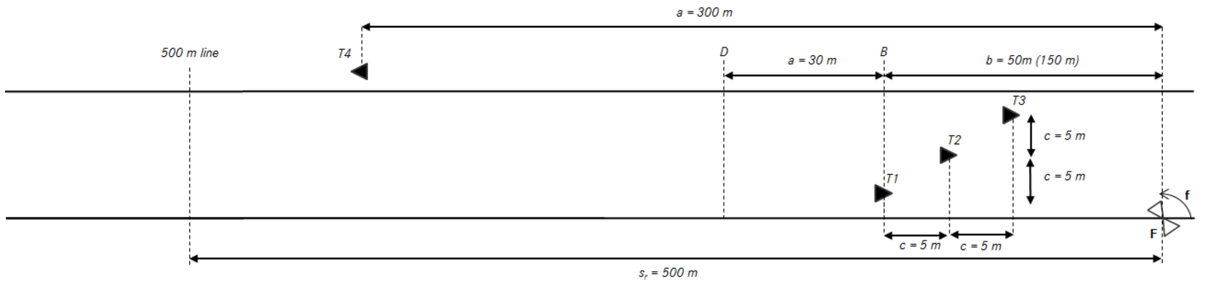


**Figure 28: Representation of the test setup**

To study the compatibility of automotive and fixed transportation infrastructure radars, the study was designed to have the vehicle as a victim and the fixed radar as an interferer. The interference of automotive radars to the fixed radar could be observed during the same tests.

**Setup for the test case fixed radar versus stationary vehicular LRR**

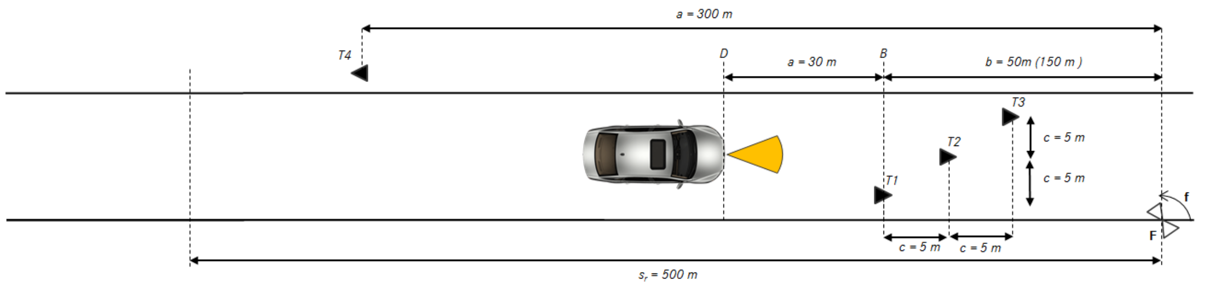


**Figure 29: Setup for the test case fixed vs stationary automotive LRR**

For stationary testing the vehicle was standing at a distance of 80 m from the fixed radar with the radar pointing into the direction of the targets and the fixed radar. These tests were repeated with the fixed radar scanning and non-scanning.

**Setup for the test case fixed radar versus dynamic automotive LRR**

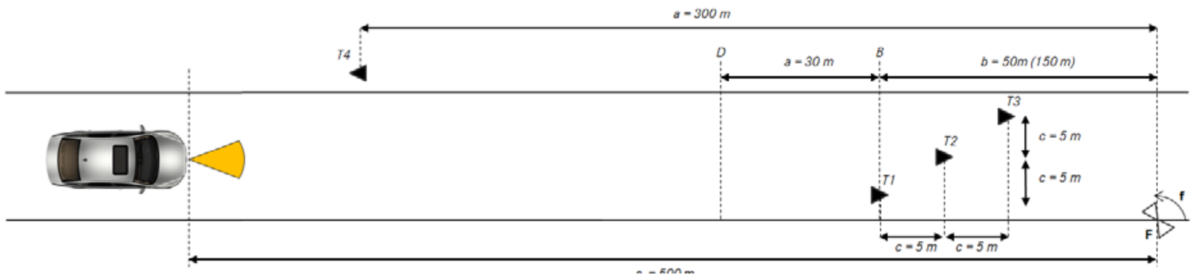


Figure 30: Setup for the test case fixed vs dynamic automotive radar

For dynamic testing, the vehicle would start its test run well outside of the 500 m field of view of the fixed radar. It would accelerate up to a speed of 60 kph before it would pass by the 500 m line and thereby enter into the field of sigt of the fixed radar. The car would then drive towards the targets and the fixed radar site at a constant speed of 60 kph until it would pass them by. Also these tests were repeated with the fixed radar scanning and non scanning.

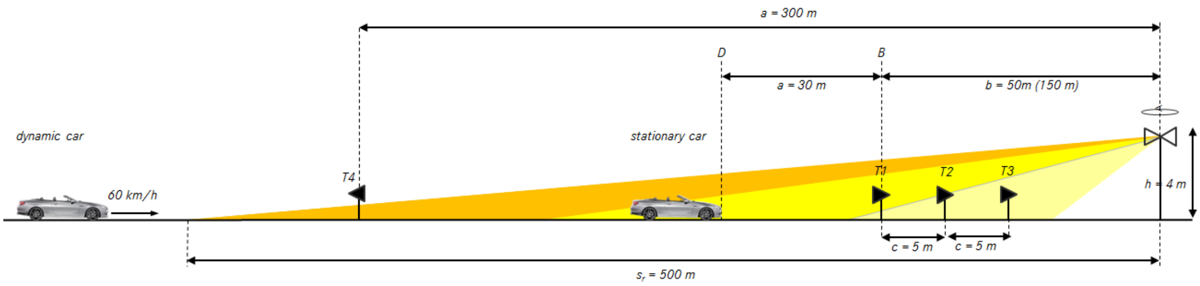


Figure 31: Sideview of the test cases fixed vs automotive radar systems

**Setup for the test case fixed radar versus automotive SRR**

For the tests of the automotive short range radar the drive pattern was adapted in order to allow reasonable testing with the side and backward looking radar system. Like with the other cases the vehicle would approach the targets at a constant speed of 60 kph. It would then pass the targets and the fixed radar by and continue driving until it would reach the 500 m line on the other end of the runway and return again over the complete distance to its initial starting position. Thereby the vehicle was illuminated from the front during the first approach and from the rear during the second approach.

**Setup for referencial vehicle vs vehicle testing**

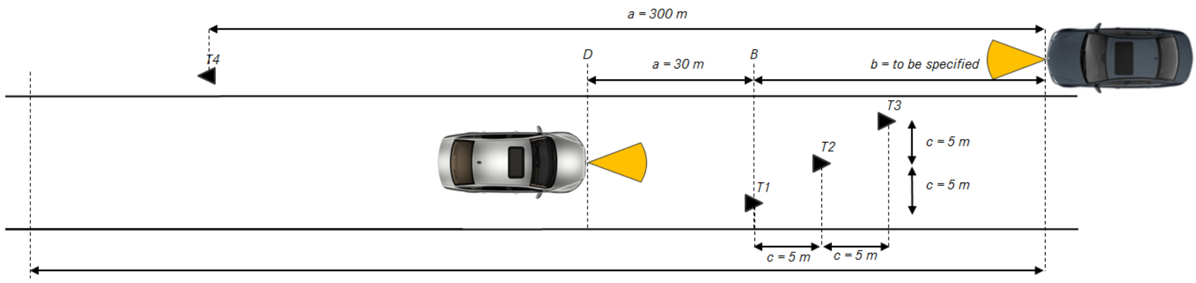


Figure 32: Setup for the referencial vehicle vs vehicle testing

### 6.1.2 Results of Neuhausen ob Eck measurements – Automotive Radar as Victim

A summary of the main Neuhausen ob Eck measurement results is given in Table 14 below.

Table 14: Results of Neuhausen ob Eck measurements

| | Automotive radar System A | Automotive radar System B | Automotive radar System C |
|---|---|---|---|
| Interference effects from measurements | Maximum noise increase to a single cycle (I+N)/N<br><br>From fixed radar<br>(F3S4 *): 11 dB<br>From other cars: 5dB | Maximum noise increase to a single cycle (I+N)/N<br><br>From fixed radar<br>(F3S4, F3D4 *): 7 dB<br>From other cars: 5dB | Maximum noise increase to a single cycle (I+N)/N<br><br>From Fixed radar (rotating): 5 dB, F3D1, F3D4<br>From other cars: 0dB |

Note 1: Automotive radar system C shows:
10 dB noise increase from fixed radar (non rotating) (F2D1, F2D2, F2D4). A non-rotating fixed radar is a non-standard operating mode and is not deployed in the field. Non-rotating mode was included in the field test to give a representation of the behaviour of non-scanning radar systems; no interference from other cars; lower interference from fixed radar compared to systems A and B. due to a dual scan concept with the use of a low bandwidth (100 MHz) for the far range scan; and confining the spectrum to within 76.0-76.5 GHz both of which effectively mitigate the interference of automotive radar and (partly) the interference by the fixed radar.

Note2: Automotive radar system B and C are high performance radar systems for high end cars and are not designed for low cost vehicles

### 6.1.3 Results of Neuhausen ob Eck measurements – Fixed Infrastructure Radar as Victim

Main observations and comments:

- Increases in noise floor were observed in some test scenarios;
- Some automotive radars produced a greater interference to the victim fixed radar than others;
- More frequent noise floor changes were observed in scenarios with non-rotating radar, however this is non-standard set up and not representative of installations along the road side. This setup does not benefit from the inherent periodic nature of the scanning radar and increases the probability of cross-correlation between systems;
- Within the scenarios tested with a rotating radar, the interference from automotive to the victim fixed radar was not enough to significantly degrade the tracking performance;
- As the number of automotive radars increase, the probability of detected interference will increase.

## 6.2 FIELD TRIAL MEASUREMENTS FROM HINDHEAD TUNNEL IN THE UK

Two automotive radar manufacturers undertook a series of measurements in a real life deployment of fixed insfrastructure radars in the UK.

- For automotive manufacturer A, measurements were made using rear corner SRR radars mounted on a vehicle that drove through the length of the 1830 m long Hindhead Tunnel several times in each direction;
- For automotive manufacturer C, Measurements were made using a front mounted LRR.

Each tunnel bore contained 6 fixed radars along its length, with mechanically rotating heads with 2 second rotation period and chirp periods of 1ms. The deployment of radars was roughly 300 m spacing.

### 6.2.1 Comparison of the fixed radar and automotive radars used during the measurements

Figure 32 shows the 41µs ramp period of the automotive SRR system compared to the 1ms slow chirp of the fixed radar. Measurements are made during the upwards slope of the signal across an 850 MHz bandwidth. The automotive radar performs 128 such ramps in rapid succession over a period of 6.5ms. The measurements are repeated each 40ms cycle. For the time instances when the automotive radar and fixed radars are of similar frequencies, we would expect to see interference in the time domain signal of the automotive radar.

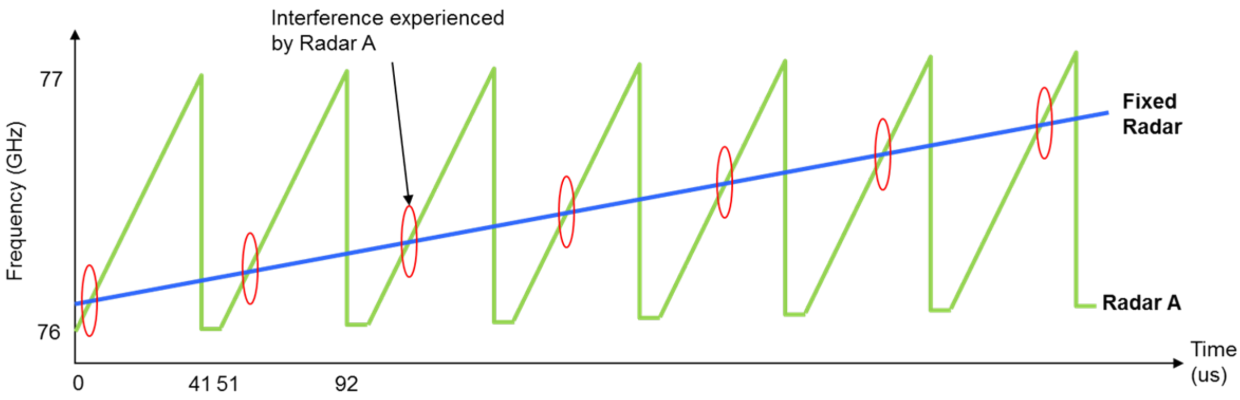


**Figure 33: Timing of the automotive radar system A versus the fixed radar**

### 6.2.2 Measurement results of Hindhead Tunnel field trials – Automotive radar as victim: Time domain

The figure below shows a series of such chirp measurements made from the sampled baseband signal, acquired during one cycle in which the interference from the fixed radar was very damaging. The x-axis of each plot represents the time domain and the y-domain represents the amplitude of the acquired signal. As can be seen, the timing of the interference burst is as expected. The rotation speed and beam pattern of the fixed radar is such that the signal is easily detectable at the start and finish of the chirps and particularly large in the middle of the chirps. This represents a worst case since the chirps are amplitude-weighted according to a window, with strongest weighting to the central chirps.

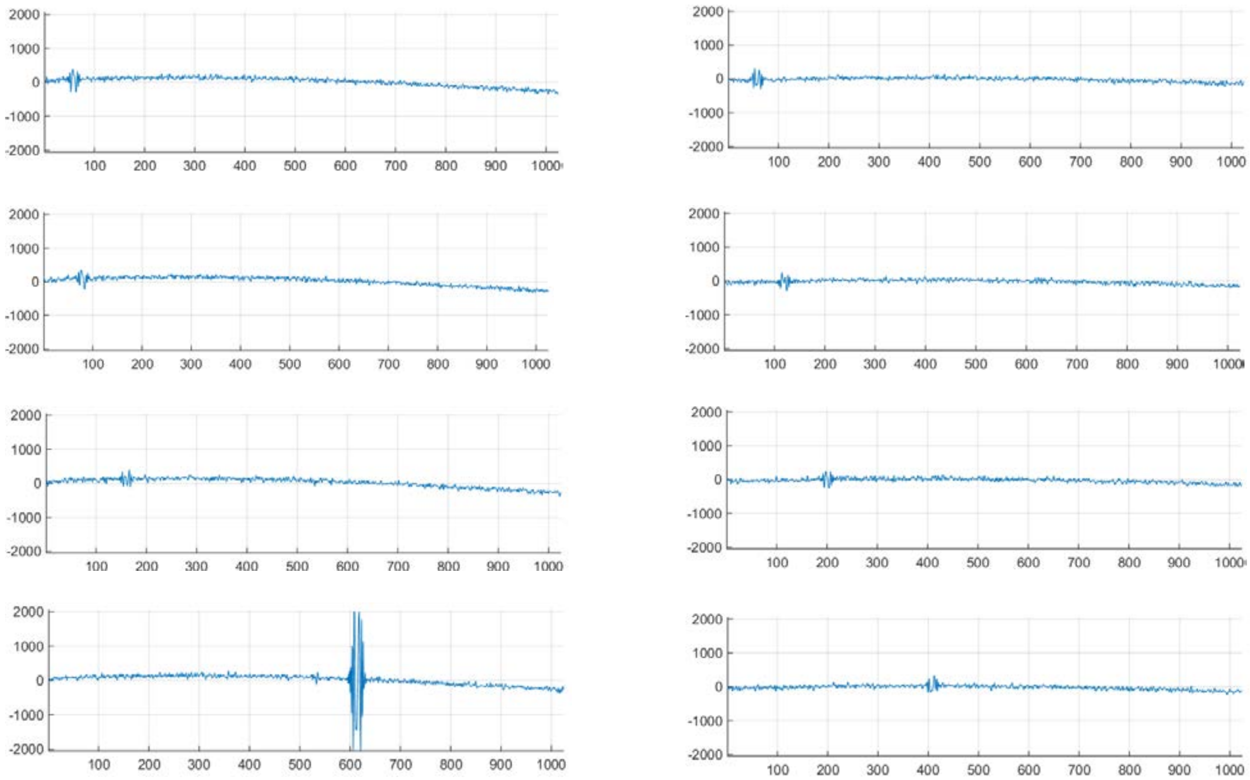

**Figure 34: Example measurements made by one radar**
**(Cycle 2628 chirps 1, 2, 3, 5, 6, 63 and 128 respectively)**

The figure below shows an example of the unwanted signal burst which illustrates the spike-like mirrored-chirp pattern described in Section 3.2.2. The unwanted signal burst looked very similar in the time domain from chirp to chirp.

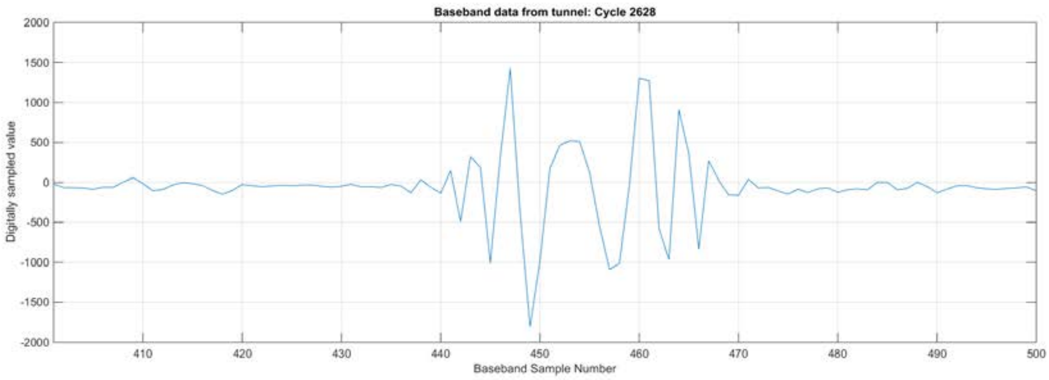


**Figure 35: Example of the unwanted signal burst which illustrates the spike-like mirrored-chirp pattern**

### 6.2.3 Measurement Results of Hindhead Tunnel field trials–Automotive Radar as Victim: Frequency Domain

The folllowing is based on the Matlab calculations of the measured signal from manufacturer A.

The automotive radar processes all the chirp signals using a windowed 2D FFT to arrive at a Range-Doppler matrix. This is represented below, where t he x-axis now represents the range bin, and the radial distance to a target can be obtained by multiplying the range bin by 0.18m. The y-axis represents the relative signal level of the signal in dB. The light green curve is an estimate of the noise at each range bin by looking at the ordered statistics of all samples in the dopper domain. At each range bin, the red curve shows the maximum value across all doppler bins, whereas the olive curve is limited to the non-stationary doppler bins.

The left hand figure shows the information obtained from cycle 2628 and the right hand figure shows cycle 2629 (which shows the more typical noise floor). In cycle 2629, no interference from the fixed radar is seen as the fixed radar is now pointing away from the automotive radar. One can see the noise floor in cycle 2628 has risen considerably such that many targets would no longer be detectable. Any such cycles of lost detections would result in delays to creation of new tracks thus slowing reaction time and would inhibit safety features. In the event of several successive cycles of similar interference levels, the automotive radar would discard all tracked objects and would give no feedback or assistance to the driver.

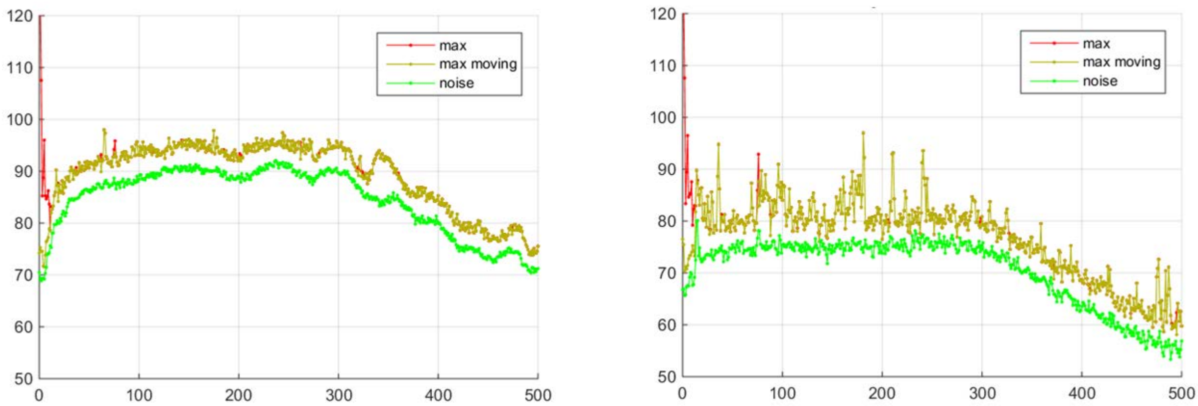


**Figure 36: Results of FFT processing on the ADC signal (Cycles 2628 and 2629)**

### 6.2.4 Measurement Results of Hindhead Tunnel field trials – Automotive Radar as Victim: Temporal Results

Each drive measurement started before the entrance to the tunnel and finished a short distance beyond the tunnel. Figure 37 **Error! Reference source not found.**shows the noise floor rise ((I+N)/N) in the y-axis and cycle number in the x axis, where each cycle has 40 ms duration.

The vehicle with left and right rear corner radars progressed at a roughly constant speed of around 60kph through the tunnel. The red curve provides an indication of the noise rise across all range bins in the stationary doppler slide, whereas the blue curve, which is more relevant, gives an indication of the noise rise across all range and doppler bins. Noise rise is calculated using a 2D median filter.

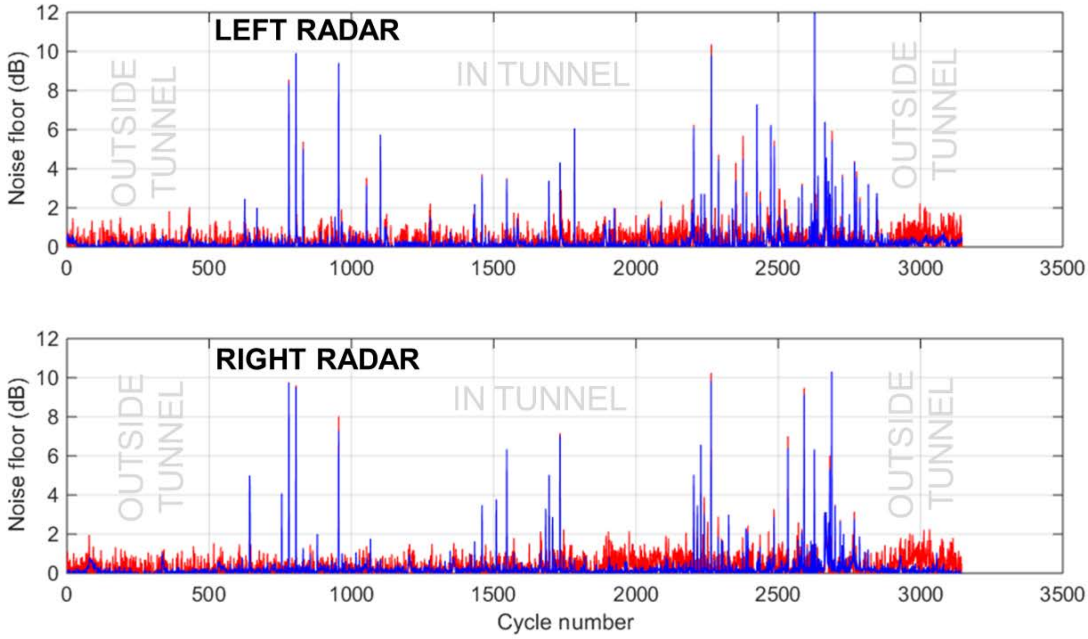


**Figure 37: Interference measurements in Hindhead Tunnel in the UK**

At the start of the measurement, the vehicle is adjacent to large concrete walls, and we enter the tunnel at cycle 200. The first fixed radar is visible from the video recording at cycle 600 and corresponds to the first set of spikes in the above figure. The large spikes at cycle 800 do not correspond to passing a fixed radar. Passing each other fixed radar results in large spikes, some of which are present before and after passing the radar and others are visible only after passing a radar. The large spike at cycle 2628 occurs 2 seconds after passing a fixed radar.

The general observations are:

- The automotive radar experiences a noise rise on the order of 10dB or more, for several cycles;
- We see that interference is only present while the vehicle is inside the tunnel. This means that the surrounding vehicles in the traffic flow were not producing measurable interference, in the open surface road environment;
- When first entering the tunnel, the interference is spaced at 25 cycles (1 second). However towards the end of the tunnel, several cycles per second experience interference. This may be due to the cumulative effects of the multiple asynchronous rotating radars in the tunnel, or reflections of the beams from the tunnel walls;
- The largest interference spikes are generally seen when close to the fixed radar.

### 6.2.5 Results of Hindhead Tunnel field trials – Fixed Infrastructure Radar as Victim

There are no results to present for the fixed infrastructure radar as a victim during the field trial in the Hindhead Tunnel. The trial was undertaken unilaterally without co-ordination with the fixed infrastructure radar supplier to allow the gathering of comparative results. In contrast to the co-ordinated activities undertaken in Neuhausen ob Eck, the field trial presented here for Hindhead Tunnel was uncontrolled in a situation without knowledge of other potential interference sources from other automotive radars in the tunnel.

### 6.2.6 Results of automotive LRR system

The LRR system used in the Hindhead Tunnel test is a lower cost version of the Automotive Radar System C as depicted in table 6, using only one scan and a bandwidth of around 460 MHz in the 76.0 to 76.5 GHz frequency range. The results are shown in

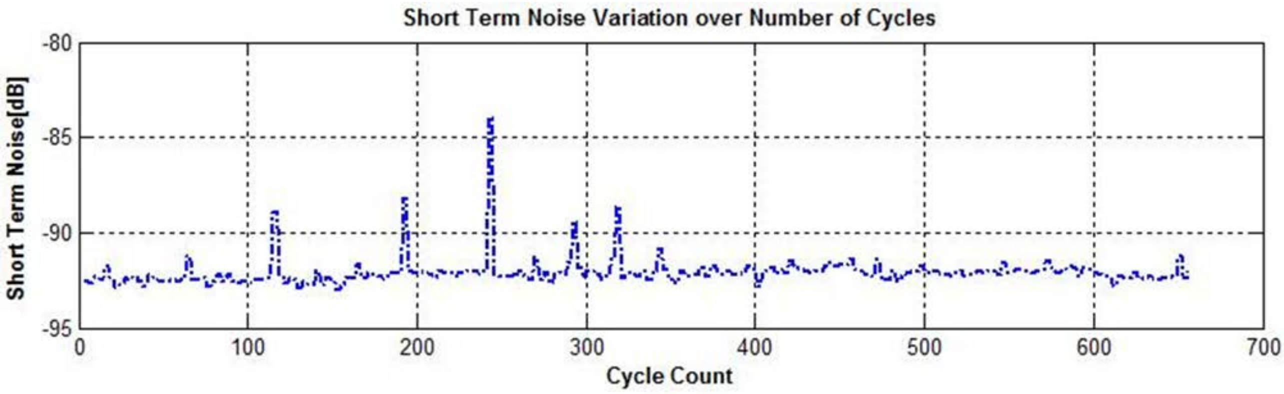


**Figure 38: Interference measurements in Hindhead Tunnel in the UK (front mounted LRR). (The interference is periodic every 25 cycles, corresponding to around 1.3 seconds each (rotation time of the 2 Hz fixed radar system))**

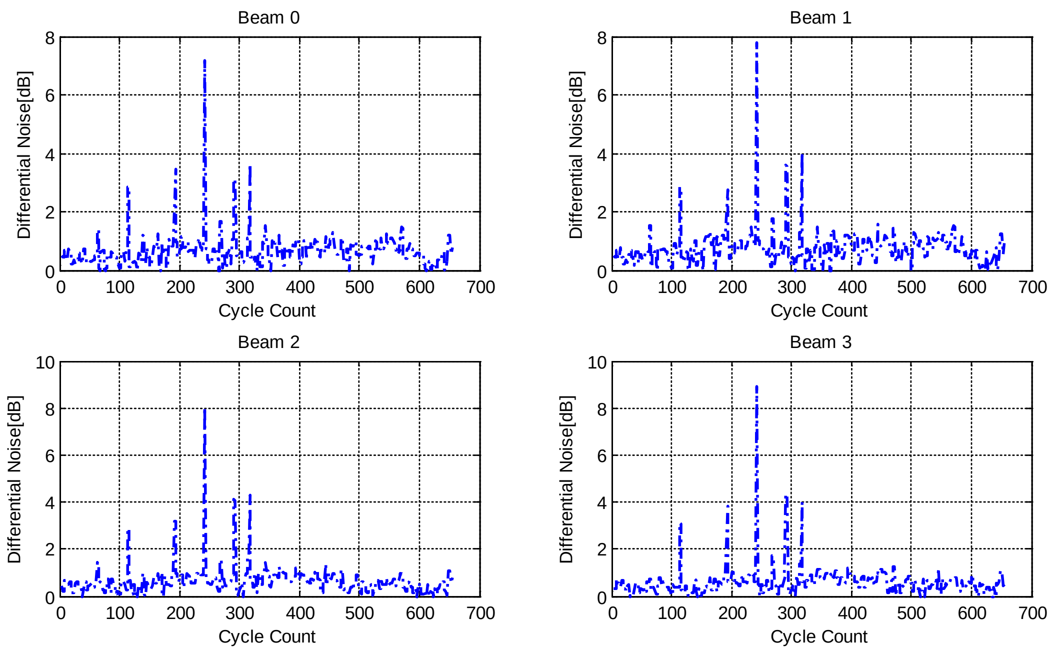


**Figure 39: Interference measurements in Hindhead Tunnel in the UK (front mounted LRR) for all angular beams (shown 0-7)**

It can be clearly seen, that the 6 fixed radars per tunnel tube result in occasional significant (10dB) increase of noise level and subsequently to reduced range in all angle beams, corresponding to a field of view (FoV) of +/-45° for this radar type, possibly due to the strong reflection from the tunnel side walls.

Note that a cycle count of 650 corresponds to a distance travelled of around 1km (at 30m/s).

During the passage through the tunnel the vehicle has been illuminated several hundred times by fixed radar beam. The majority of these illuminations have produced no effect. This may be due to duty cycle and timing effect.

The 10 dB increase in noise level indicate similar results to those seen during the Neuhausen test scenarios F2 (rotation of fixed radar stopped). Propagation effects for this sort of signals in tunnels are not fully understood.

# 7 DISCUSSION AND ANALYSIS

**Effects that can worsen the interference situation**

Some effects were not considered in the theoretical and practical studies which could impact the results (see Table 15)

**Table 15: Further factors which may affect the interference potential**

| Effect | Description | Impact on interference |
|---|---|---|
| Aggregated effect from several fixed radars | For monitoring a long road section, a fixed radar installation is needed nominally every 500 m. | Probability for negative interference impact increases as multiple cycles affected per second. |
| Proliferation of fixed radars to other areas | Monitoring of areas close to roads with fixed radars cannot prevent waves from reaching the road. | Probability for negative interference impact increases as multiple cycles affected per second. However increased distance of the fixed radar from road will reduce the effect. |
| Higher propagation path loss due to bad weather | Higher path loss effects the victim radar measurement twice while it effects interference signal only once. This effect is symetrical and is true of a situation with Fixed radar as victim from automotive radars. | Reduced target C / I resulting in lower detection probability. |
| Influence of environment near the fixed and automotive radar | Clusters due to sidelobes of the fixed and automotive radar can occur due to nearby objects. This is significant if the fixed radar is physically close to the automotive radar. | Additional desensitisation of automotive radar possible when near to fixed radar. This is due to the Minimum Coupling Loss (MCL) being reduced. |
| Proliferation of automotive radars | Increasing the number of automotive radars will lead to a greater density of 76-77 GHz radars on the roads. | Probability of interference between vehicles and fixed infrastructure radars. |

## 7.1 TIME-DOMAIN BASE-BAND SIGNALS AT THE OUTPUT OF THE BANDPASS FILTER

### 7.1.1 General remarks

The combination of the downconverter and the bandpass filter means that interfering signals are only passed through if the frequency offset between the interfering signal and the victim LO signal falls within the pass bandwidth of the filter. Typical values for automotive radar sensors as victims are given as “Rx IF bandwidth (after signal processing)” in Table 3.

The time-domain signal shape at the bandpass filter output can in principle be computed analytically, but here a more simplified simulation approach is taken by only testing whether the difference of down-converter input frequencies passes through the bandpass filter, and used to simulate different scenarios of victim and interferer modulations (see next section).

Not considered here is the possible effect, that interference in principal can also cause nonlinear distortion in the victim downconverter or bandpass filter if the interference power is larger than the victim Rx RF or victim Rx IF 1dB compression points. The consequence of such distortion would be degraded Noise Figure and the generation of higher harmonics, meaning additional parasitic peaks in the FFT spectrum. But comparing the interference power levels from the simulation in section 3.1 with the respective 1dB-compression data in Table 3 gives, that nonlinear distortion can be neglected here for the following considerations.

### 7.1.2 Simulation results

Seven scenarios are considered with different combinations of fast and slow chirps and different centre frequencies. Here, the FSR uses slow chirp modulation, while the automotive victim uses slow chirps or fast chirps.

In each scenario described below the victim and interferer sweep parameters are described as well as any start time offset between the two swept sources. These parameters with the default values are shown below:

1. Start Frequency, default 76 GHz;
2. Swept Bandwidth, default 500 MHz;
3. Sweep Time, default 625 µs.

Below the parameters there are two graphs:

1. N sweeps are shown to illustrate df/dt for the victim and interferer, relative to each other;
2. IF chain voltage changes due to received interference signal within the receiver Bandwidth. The graph does not calculate the actual IF voltage level, but simply indicates the presence of signal within that receiver bandwidth set in the parameters of the victim radar.

**Table 16: Scenario 1 - Two sweeps with the same swept BW and sweep time but a small change in start time**

| Parameters of victim radarn | | Parameters of interfering radar | |
|---|---|---|---|
| Start Freq (GHz) | 76.0 | Start Freq (GHz) | 76.0 |
| Swept Freq (MHz) | 500 | Swept Freq (MHz) | 500 |
| Chirp Time (µs) | 625 | Chirp Time (µs) | 625 |
| IF BW (MHz) | 5 | Time Delay Interferer to victim (µs) | 1 |


**Figure 40: Victim and interferer chirps over time**

The IF signal in the victim radar.

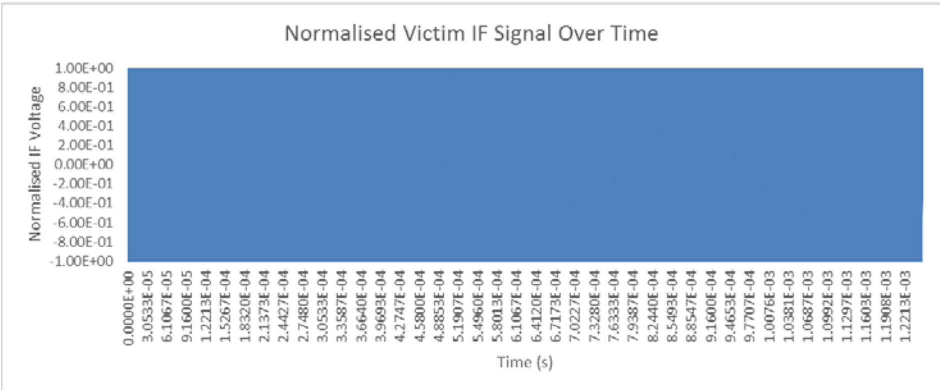


**Figure 41: Normalised victim IF signal over time**

Scenario 1 observation:

There will be a continuous wave IF signal due to the interference as long as the time delay is short enough for the beat frequency to be less than the IF bandwidth of the victim. The IF signal will appear as a single frequency and hence the interference will all fall within the same range bin thus creating a false raw target. If the false raw target is present in a consistent Range-Doppler cell across successive cycles, then a false object will be created by the tracker. Employing timing or frequency jitter can ensure false targets cannot be created.

**Table 17: Scenario 2 - Two sweeps with the same swept BW and sweep time but a small change in start time**

| Parameters of victim radarn | | Parameters of interfering radar | |
|---|---|---|---|
| Start Freq (GHz) | 76.0 | Start Freq (GHz) | 76.0 |
| Swept Freq (MHz) | 500 | Swept Freq (MHz) | 500 |
| Chirp Time (µs) | 625 | Chirp Time (µs) | 625 |
| IF BW (MHz) | 5 | Time Delay Interferer to victim (µs) | 10 |


Figure 42: Victim and interferer chirps over time

The IF signal in the victim radar.

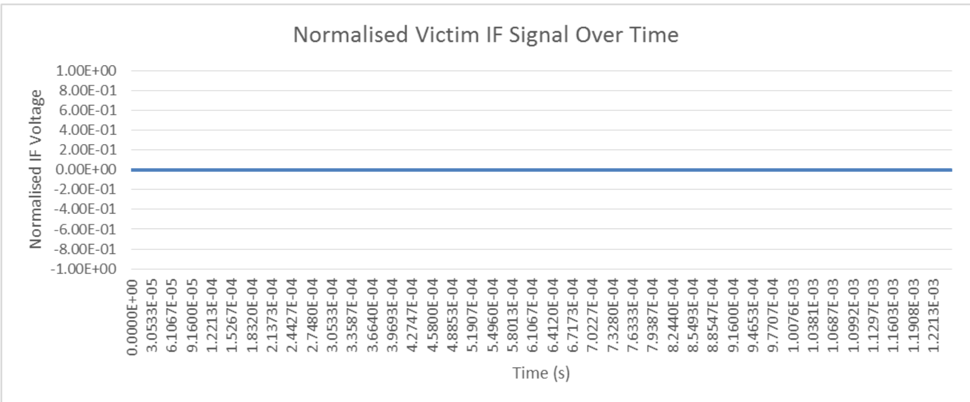


Figure 43: Normalised victim IF signal over time

Scenario 2 observation:

A small change in start time results in the beat frequency falling outside of the receiver IF BW resulting in no IF signal and no interference.

**Table 18: Scenario 3 - Two sweeps with the same swept BW and almost same sweep time**

| Parameters of victim radarn | | Parameters of interfering radar | |
|---|---|---|---|
| Start Freq (GHz) | 76.0 | Start Freq (GHz) | 76.0 |
| Swept Freq (MHz) | 500 | Swept Freq (MHz) | 500 |
| Chirp Time (μs) | 250 | Chirp Time (μs) | 260 |
| IF BW (MHz) | 5 | Time Delay Interferer to victim (μs) | 1 |

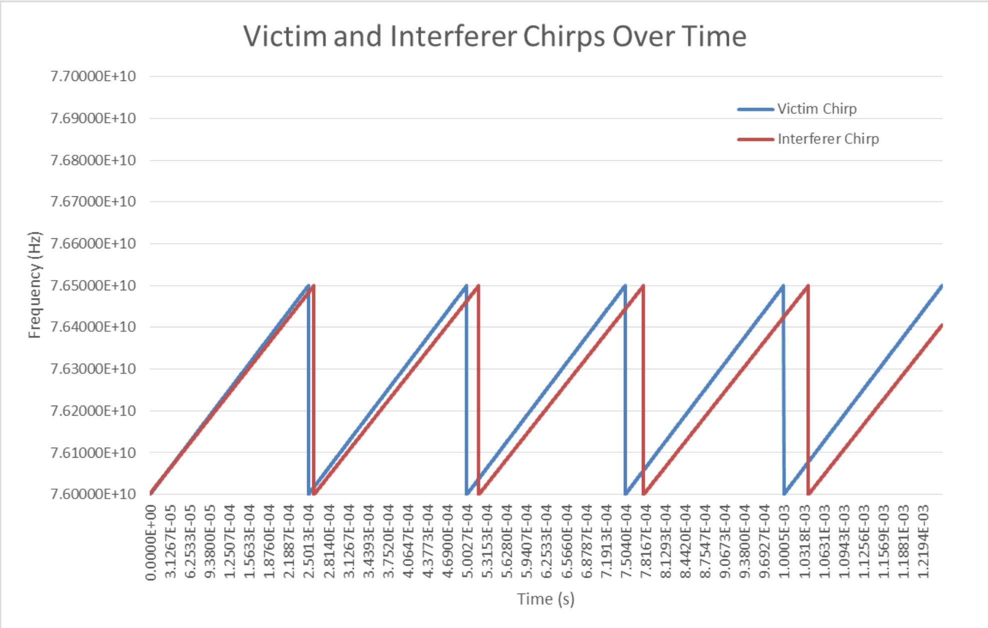


**Figure 44: Victim and interferer chirps over time**

The IF signal in the victim radar.

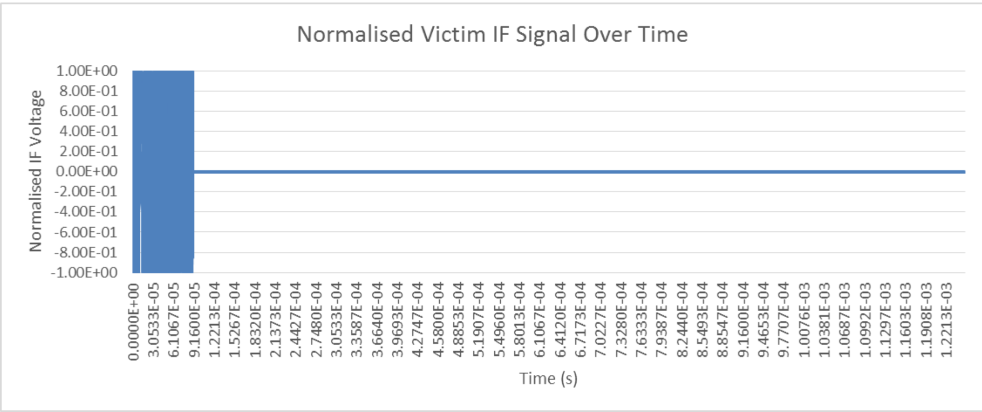


**Figure 45: Normalised victim IF signal over time**

Scenario 3 observation:

Spike-like interference is seen only for a very short time. The interference will not be observed for several chirps.

**Table 19: Scenario 4 - Two sweeps - one fast chirp, one long chirp showing the points of interference**

| Parameters of victim radarn | | Parameters of interfering radar | |
|---|---|---|---|
| Start Freq (GHz) | 76.0 | Start Freq (GHz) | 76.0 |
| Swept Freq (MHz) | 500 | Swept Freq (MHz) | 500 |
| Chirp Time (µs) | 40 | Chirp Time (µs) | 625 |
| IF BW (MHz) | 5 | Time Delay Interferer to victim (µs) | 1 |

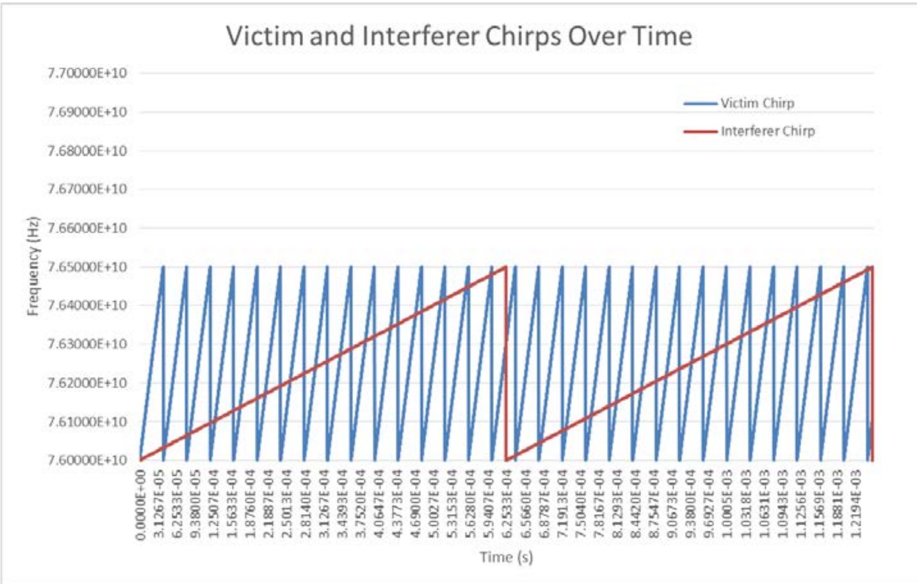


**Figure 46: Victim and interferer chirps over time**

The IF signal in the victim short chirp radar.

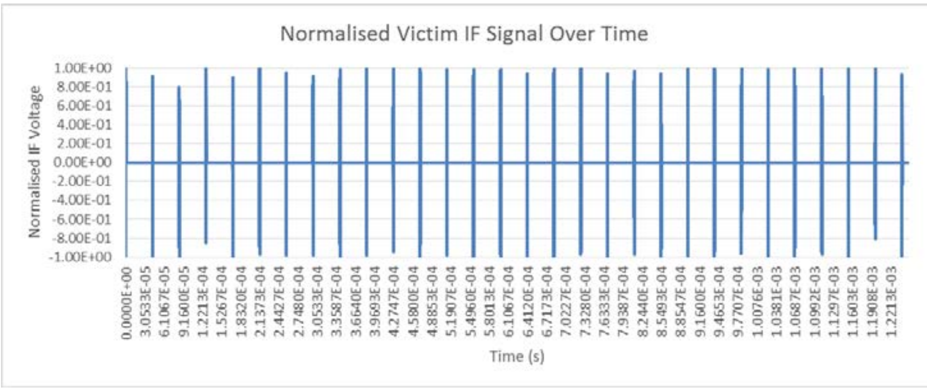


**Figure 47: Normalised victim IF signal over time**

Scenario 4 observation:

There will be one spike-like interference in the IF signal of the Victim radar per chirp, as the victim's receiver scans past the interferer. The difference between the frequencies will reduce rapidly from the IF bandwidth when the signal is first detected, down to DC, then back to the IF bandwidth before being disappearing. This "mirrored chirp" will appear at different times within the chirp measurement. Due to the nature of the mirrored chirp signal, it will be spread over the whole measurement bandwidth of the receiver. The amplitude of this "mirrored chirp" increases and decreases in amplitude according to the baseband filtering characteristics.

**Table 20: Scenario 5. Two sweeps – Fast sweep and slow sweep occupy a partially overlapping band**

| Parameters of victim radarn | | Parameters of interfering radar | |
|---|---|---|---|
| Start Freq (GHz) | 76.0 | Start Freq (GHz) | 76.125 |
| Swept Freq (MHz) | 500 | Swept Freq (MHz) | 500 |
| Chirp Time (μs) | 40 | Chirp Time (μs) | 625 |
| IF BW (MHz) | 5 | Time Delay Interferer to victim (μs) | 1 |

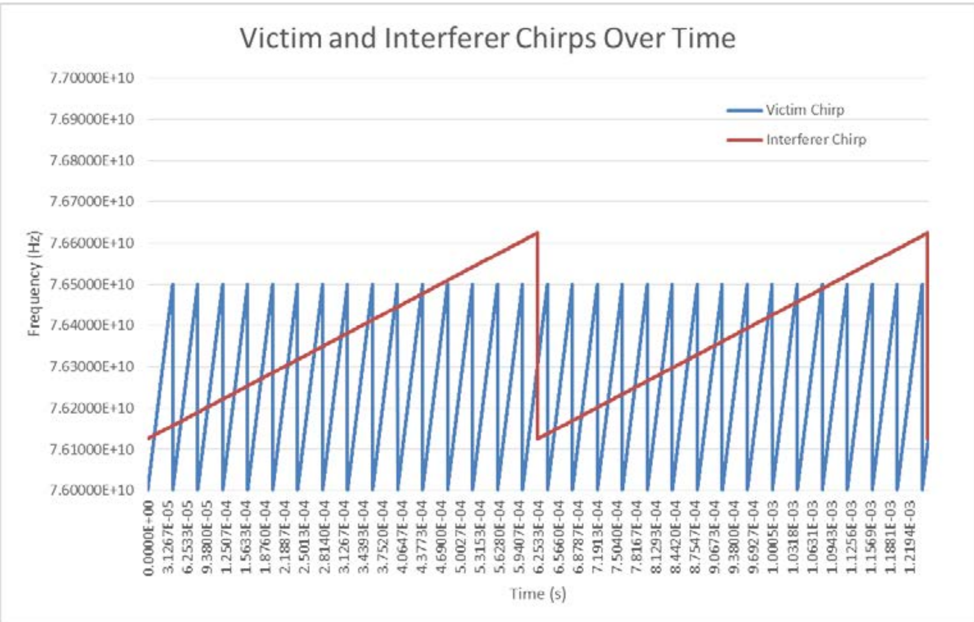


**Figure 48: Victim and interferer chirps over time**

The IF signal in the victim short chirp radar.

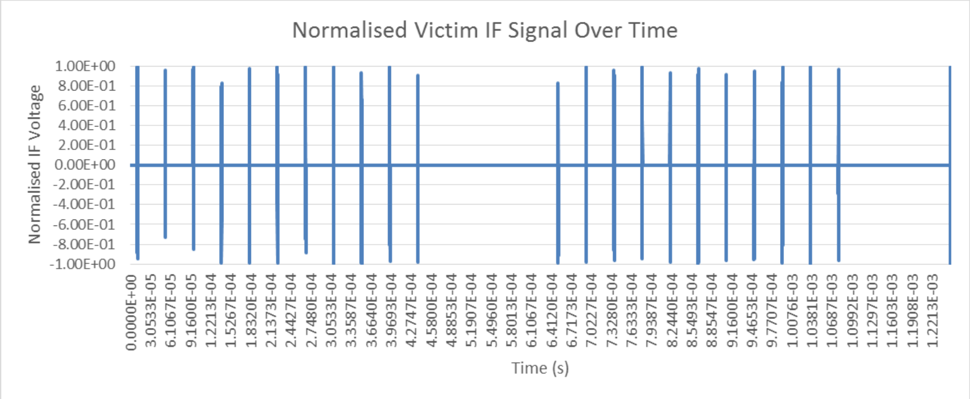


**Figure 49: Normalised victim IF signal over time**

Scenario 5 observation:

Spike-like interference will be observed for the time when the swept bandwidths overlap.

**Table 21: Scenario 6. Two sweeps - one fast chirp, one long chirp showing the points of interference, with the long chirp radar as the victim**

| Parameters of victim radarn | | Parameters of interfering radar | |
|---|---|---|---|
| Start Freq (GHz) | 76.0 | Start Freq (GHz) | 76.0 |
| Swept Freq (MHz) | 500 | Swept Freq (MHz) | 500 |
| Chirp Time (µs) | 625 | Chirp Time (µs) | 40 |
| IF BW (MHz) | 5 | Time Delay Interferer to victim (µs) | 1 |

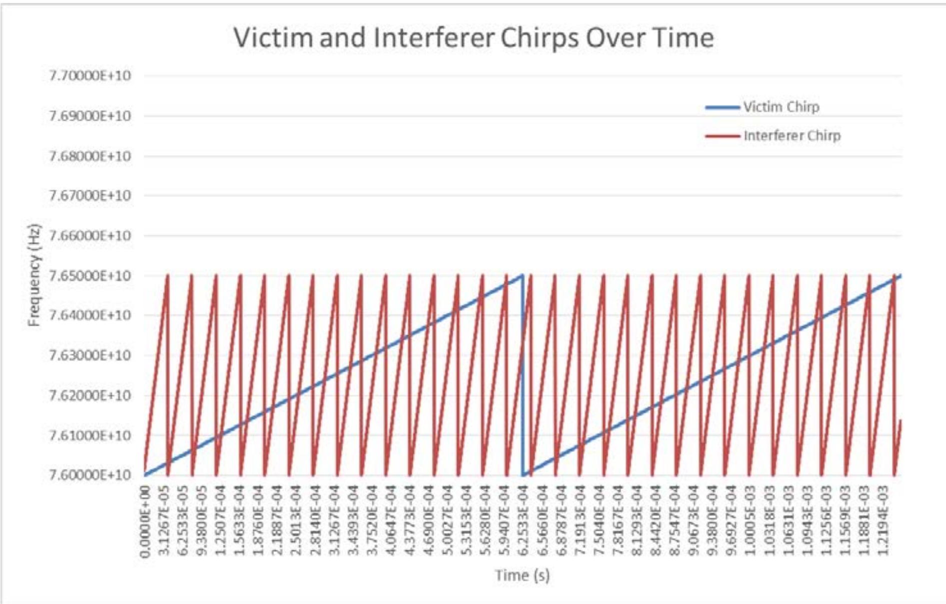


**Figure 50: Victim and interferer chirps over time**

The IF signal in the long chirp victim radar.

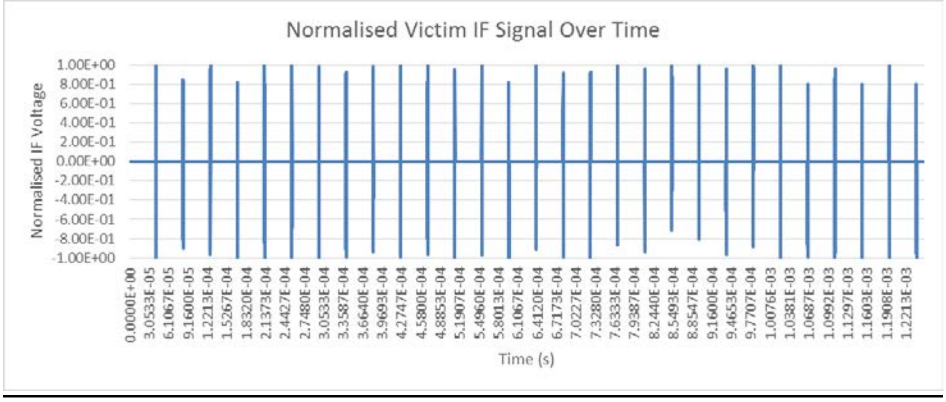


Figure 51: Normalised victim IF signal over time

Scenario 6 observation:

Spike-like interference will be observed in the long chirp victim radar for the time when the swept bandwidths overlap.

Table 22: Scenario 7. Two sweeps - one fast chirp, one long chirp each occupying non-overlapping 500 MHz Bandwidths

| Parameters of victim radarn | | Parameters of interfering radar | |
|---|---|---|---|
| Start Freq (GHz) | 76.0 | Start Freq (GHz) | 76.5 |
| Swept Freq (MHz) | 500 | Swept Freq (MHz) | 500 |
| Chirp Time (µs) | 40 | Chirp Time (µs) | 625 |
| IF BW (MHz) | 5 | Time Delay Interferer to victim (µs) | 1 |

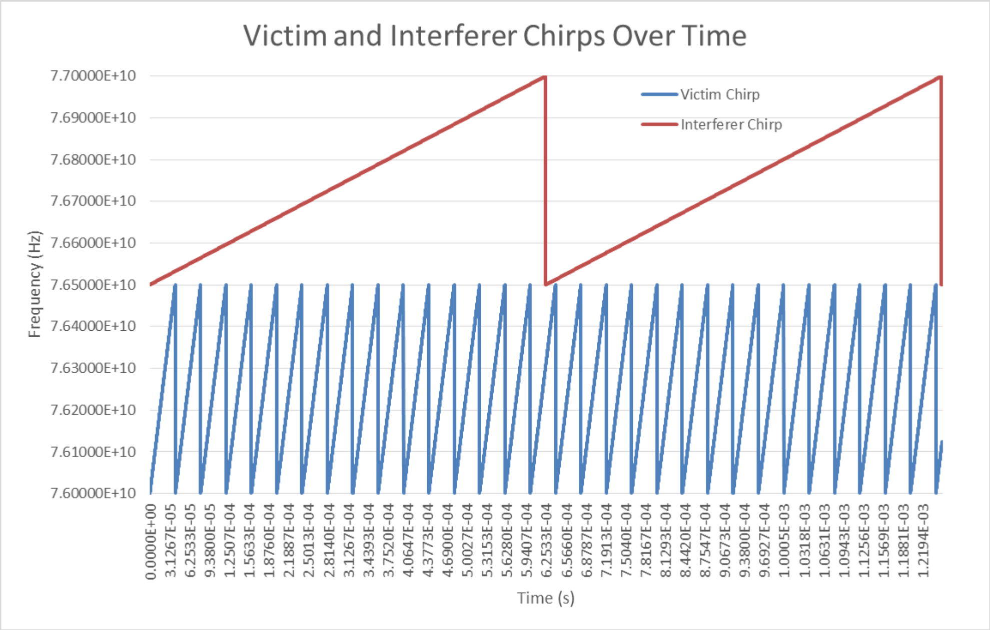


Figure 52: Victim and interferer chirps over time

The IF signal in the long chirp victim radar.

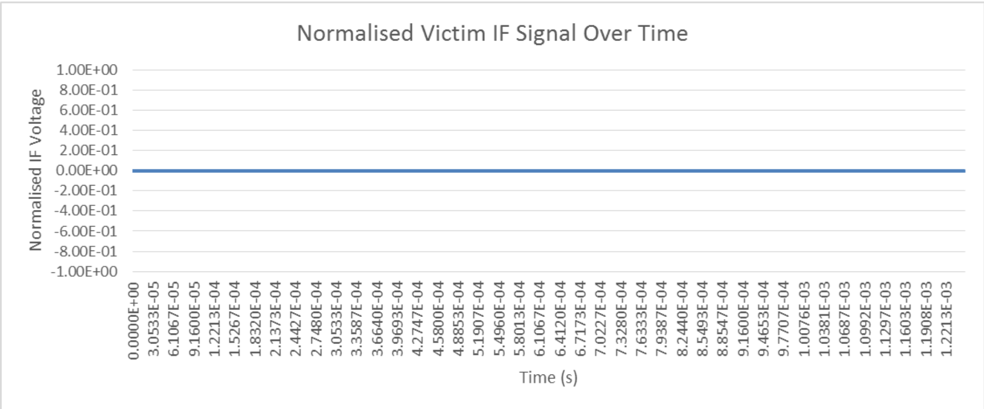


Figure 53: Normalised victim IF signal over time

Scenario 7 observation:

When the occupied bandwidths do not overlap, no interference is observed in the IF.

### 7.1.3 Modulation gain

From the shown simulation examples, it becomes obvious that the downconverter and bandpass filter can suppress part of the interference power. To describe the degree of suppression, here the modulation gain is introduced and defined as:

Modulation gain = 10*log(2*IF_bandwidth_Victim/Modulation_bandwidth_Interferer)

It is noted that the interference power alone is not sufficient to completely describe interference effects, but additionally the time-dependency is important to be considered.

## 7.2 TIME-DOMAIN SIGNAL AT THE OUTPUT OF THE ADC

The ADC has two contributions relevant for the interference effect:

a) The ADC converts a limited voltage range to a limited range of numbers. If the voltage range or the number range is exceeded, then clipping of the signal occurs. The consequence of such distortion would be the generation of higher harmonics, meaning additional parasitic peaks in the FFT spectrum. But comparing the interference power levels shown in section 3.1 with the respective 1dB-compression data in Table 3 gives, that nonlinear distortion can be neglected here for the following considerations.

b) As described in Table 4, an automotive radar sensor typically uses a periodic sequence of active measurement and result processing. ADC samples are only taken during the active measurement phase. During the processing time, no samples are taken and during that phase the victim therefore is not vulnerable to interference (see also Figure 54).

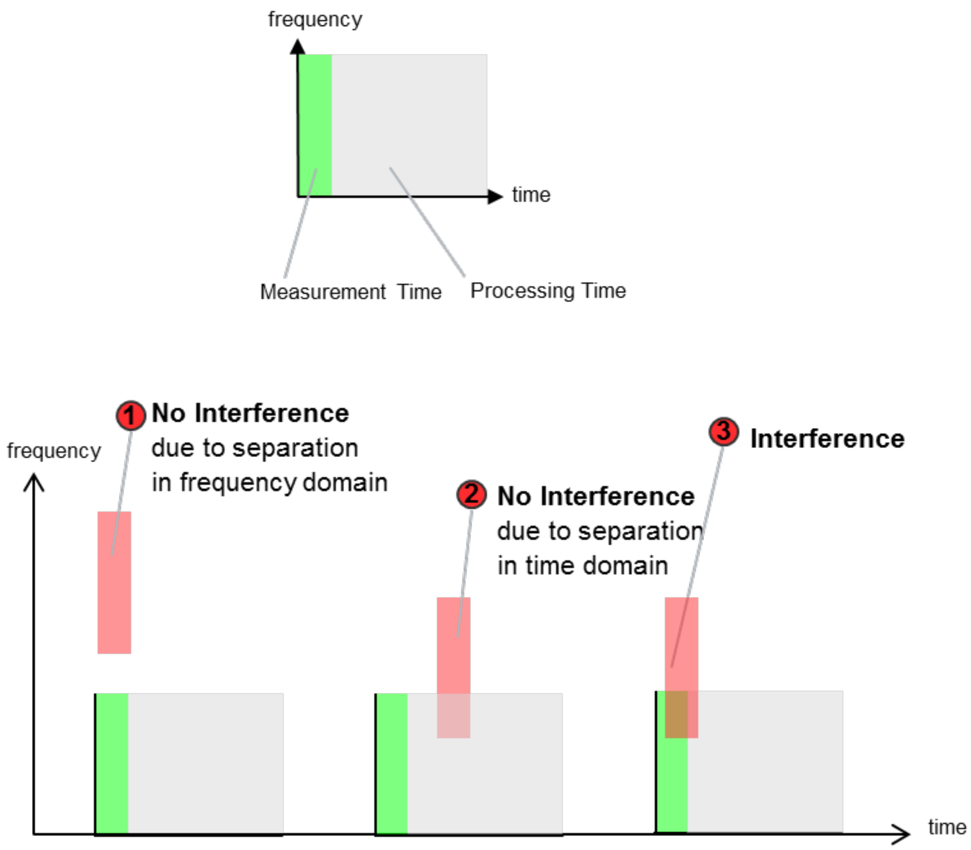


**Figure 54: Occurrence of interference depending on used bandwidth and timing**

Observation:

Interference power available at the victim receiver input and with a frequency suitable to be down-converted for passing through the victim bandpass filter can only reach the output of the ADC if the victim is actually sampling during that time.

As example, two automotive radars using exactly the same part of the band and with duty cycle of 25% may not experience any overlap of signals in the time domain as they pass each other. In this case, in 50% of occasions they would not overlap in time at all. The degree of overlap determines the extent of the possible interference in the event that the frequency ramps also cross.

## 7.3 FREQUENCY-DOMAIN SIGNAL AT THE OUTPUT OF THE FFT

### 7.3.1 General remarks

The baseband signal, which is the product of mixing the receiver signal with the local signal, is first filtered by an anti-aliasing filter and then sampled using a ADC. The anti-aliasing filter characteristics are important to avoid under-sampling of distant objects that can cause range ambiguity.

The sampled signal from each chirp is processed using a windowed FFT. The FFT provides a processing gain due to the bandwidth compression, from the ADC sampling bandwidth to the IF bandwidth represented by each bin of the FFT output, thus improving the S / N. The output vector from the FFT represents the amount of signal power returned within in each “range bin”.

FFT processing gain = 10 log (FFT-size / 2)

Each real target creates in the time domain a truncated sinusoid signal which is converted by the FFT into a peak in the spectrum.

If the sampled signal contained additional unwanted signals such as interference, then they would also be processed by the FFT as follows:

- A time-domain sine wave converts to a peak in the FFT spectrum, and would appear like a real target;
- A time-domain spike leads to broadband noise in the FFT spectrum, increasing the noise floor, and thus reducing the S / N for targets, resulting in a reduced sensitivity of the victim radar sensor;
- A time-domain burst which has the form of a mirrored-chirp signal creates interference across the IF band, reducing the sensitivity of the victim radar sensor across most range bins.

Fast-chirp FMCW radars generally transmit a series of chirps close together in order to increase the observation period and to sample the phase progression of each target. Having performed the first windowed-FFT on each chirp, a second windowed-FFT is then performed on each range bin in order to aggregate the data from all chirps. This results in a 2D matrix, with range bin (radial distance) in the x-dimension and target speed (Doppler) in the y-dimension.

The second FFT provides a further processing gain due to the extension of the observation period. However, the levels of the resulting 2D noise floor may also be clustered due to any of the following aspects:

- If the interference burst signal is similar from chirp to chirp, albeit at different positions in each chirp. A degree of similarity would be expected in the event that the victim and interferer slopes are kept constant;
- If the interference burst moves within the time domain in a deterministic way. For example, interference from a slow chirp interferer that is present in each chirp measurement of a fast chirp system, where the burst progresses in a deterministic way through the samples of the baseband signals.

### 7.3.2 Noise increase analysis including processing and modulation gain - Automotive Radar as Victim

The relevant details of some exemplary systems are given in Table 23

**Table 23: Summary of sensor details**

| | Automotive radar system A | Automotive radar System B | Automotive radar[1] System C[2] | Fixed radar system |
|---|---|---|---|---|
| Type | Fast chirp | Slow chirp | Fast chirp | Slow chirp |
| Sensor | Rear Corner | Front Centre | Front Centre | Fixed Infrastructure Radar |
| Antenna polarization | Vertical | Vertical | Horizontal | Horizontal |
| Antenna beam width azimuth (-3dB) | Rx: 120° | Rx: 90° | +/-2.4° (Rx far scan) | Tx: 1.8°, rotation speed: 360° in 0.25 s to 1 s |
| Max. antenna gain | Rx: 14 dBi | Rx: 20 dBi | 25 dBi (Rx far scan) | |
| Tx feed power | / | / | / | 10 dBm |
| Modulation | FMCW | FMCW | FMCW | FMCW |
| Chirp duration | 40µs | 1-10 ms | 25 µs (Rx far scan) | 1 ms |
| Measurement bandwidth | 850 MHz | 500 MHz | 100 MHz (far scan) | 600 MHz |
| IF bandwidth | 12.5 MHz | 500 kHz | 5 MHz | / |
| Rx noise figure NF | 14 dB | 15 dB | 15 dB | / |
| FFT size (number of samples) | 1024 samples per chirp *64 chirps | 256 samples per chirp | 256 samples * 512 chirps (far scan) | |

Table 24 provides a summary of I (Interference power) and N (noise power) along important processing steps in typical automotive radar Rx chain up to FFT output, in order to better understand the noise increase effects on the automotive radar side.

[1] Automotive radar system C provides an additional feature of near scan, however, the related parameters were not used in the studies.

**Table 24: Summary of I and N along fundamental processing steps of typical vehicular radar Rx chain up to FFT**

| Position in victim Rx chain | Interference power I | Noise power N |
|---|---|---|
| **Antenna feed point** | Superposition of direct path between interferer and victim with indirect paths like for example reflection on road surface or reflection on tunnel wall | Thermal noise considered, galactic noise neglected. |
| **Polarisation gain**: | ≈10dB for the case of cross-polarisation | |
| **Down-converter** | Down-conversion gain | Noise figure of FMCW radar is set by source noise, not noise figure |
| **IF filtering output** | **Modulation gain:**<br>FMCW of victim and interferer only cross for limited amount of time.<br>10*log(2*IF_bandwidth_Victim/Modulation_bandwidth_Interferer) | Limitation of thermal noise power:<br>-114 dBm/MHz +10log(2*IF_bandwidth_Victim/MHz)+NF |
| **AD conversion output** | AD can be forced into compression by spikes in IF | Power supply noise and sampling noise neglected here. |
| **FFT output** | **Processing gain:**<br>Spike-like interference power is converted into broad-band noise.<br>10log(FFT size_victim/2)<br>No valid physical mechanism for this due to an FFT | **Processing gain:**<br>White noise is distributed amongst narrow Range-Doppler bins by the FFT process:<br>10log(FFT size_victim/2) |

Two simplified static interference scenarios are introduced below:

- Example “long distance”:
  - The car radar sees in that distance the max fixed radar gain with its max gain;
  - A distance of 100m is assumed;
- Example “short distance”:
  - Car radar in 7m distance to the fixed radar;
  - Fixed antenna with 0 dBi assumed, car antenna with -10 dBi.

Table 25 is then calculating the noise increase at the two auromotive radar systems from the fixed radar for those two scenarios when using the  receiver processing steps as in Table 24 above.

**Table 25: Impact of fixed radar on automotive radars**

| | Automotive radar system A | Automotive radar System B | Automotive radar System C | Remarks |
|---|---|---|---|---|
| A: Example long distance, Calculated interference power at automotive radar Rx antenna feed point | I_11 = -56dBm | I_l1 = -50dBm | I_l1 = -50dBm (far scan) | 100m, path loss 110dB, Tx feed power 10dBm, Gt=max. gain, Gr=max. gain. Indirect paths neglected. |
| B: Example short distance, Calculated interference power at automotive radar Rx antenna feed point | I_s1 = -87dBm | I_s1 = -87dBm | I_l1 = -87dBm (near scan) | 7m, path loss 87dB, Tx feed power 10dBm, Gt=0dBi, Gr=-10dBi. Indirect paths neglected. |
| C: Polarisation gain | -10dB | -10dB | 0dB | |
| D: Down-conversion gain | 0dB | 0dB | 0dB | Arbitrary choice because interference and noise are influenced identically |
| E: Modulation gain | 10*log (2*12.5/600) = -13.8 dB | 10*log (2*0.5/600) = -27.8 dB | 10*log (2*5/600) = -17.8 dB | |
| **F: Resulting interference power after IF filtering** | **I_l2 = -81dBm I_s2 = -112dBm** | **I_l2 = -89dBm I_s2 = -126dBm** | **I_l2 = -69dBm I_s2 = -106dBm** | **A+C+D+E B+C+D+E** |
| G: Thermal noise power after IF filtering | -114+10log(25) +14=-86dBm | -114+10log(1) + 15=-99dBm | -114+10log(10)+ 15=-89dBm | |
| H: Processing gain | -10log (1024*64/2) = -45 dB | -10log (256/2) = -21 dB | -10log (256*512/2) = -48 dB | |
| I: Resulting interference noise power after FFT | I_l3 = -126dBm I_s3 = -157dBm | I_l3 = -110dBm I_s3 = -147dBm | I_l3 = -117dBm I_s3 = -154dBm | F+H |
| J: Resulting thermal noise power after FFT | -131dBm | -120dBm | -137dBm | G+H |
| **K: I/N long distance short distance** | 5 dB -26dB | 10dB -27dB | 20dB -17dB | I-J |
| **Noise increase (I+N)/N long distance short distance** | 6 dB 0.01dB | 10dB 0.01dB | 20dB 0.1dB | 10log(1+10^(K/10)) |

The calculations above contain simplifications and uncertainties and can only give a relatively coarse indication.

## 7.4 SIGNAL PROCESSING ASPECTS

The 1D or 2D FFT output from each Rx channel are processed to identify a list of features (detections) that are present in the observation of that particular cycle. This is generally performed by applying an amplitude threshold to remove noise, then using a local maxima search.

The level of the threshold may be kept at a constant level across all range bins by analysing the signal globally and ensuring a threshold is found that minimises false detections. Alternatively, a threshold may be defined for each bin by observing the signal level in the bins surrounding the bin and defining a level accordingly (known as CFAR).

In the case of a raised noise floor in the 1D or 2D signal due to interference:

- White noise will result in a uniform raising of the noise floor;
- Clustered noise also reduces sensitivity, but not uniformly and incurs the risk of creating false detections depending on how the threshold is calculated.

The following diagram gives an illustration of the maximum range performance for a defined target size for a given impairment to the S/N. A 12dB noise rise reduces in half the maximum detection range.

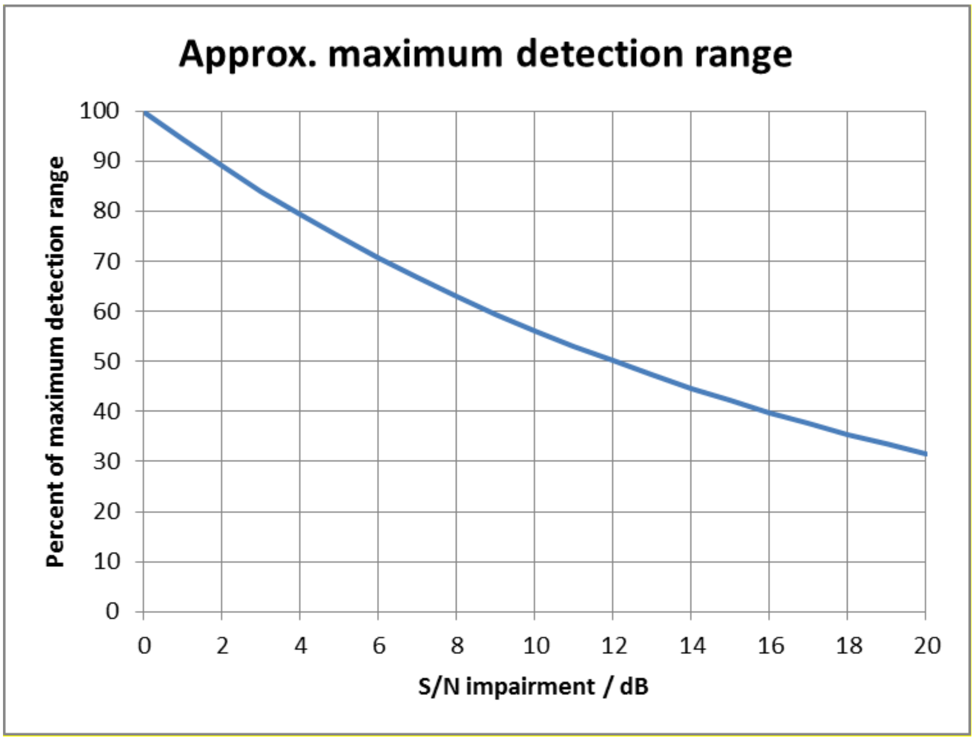


Figure 55: Reduction of maximum range as experienced by a radar due to reduction in S/N

Radars using slow chirps are less affected and often use multiple slow chirps to resolve some range-doppler ambiguity problems. If one of these is damaged, then the effect on radar processing is more subtle.

## 7.5 SYSTEM LEVEL ASPECTS

While before only interference to a single radar cycle was considered, here it is now considered that a victim sensor normally uses the information from several cycles to generate an output to the vehicle (like steering, accelerating, breaking) or to the driver (like a warning).

The following figure gives a generalized overview.

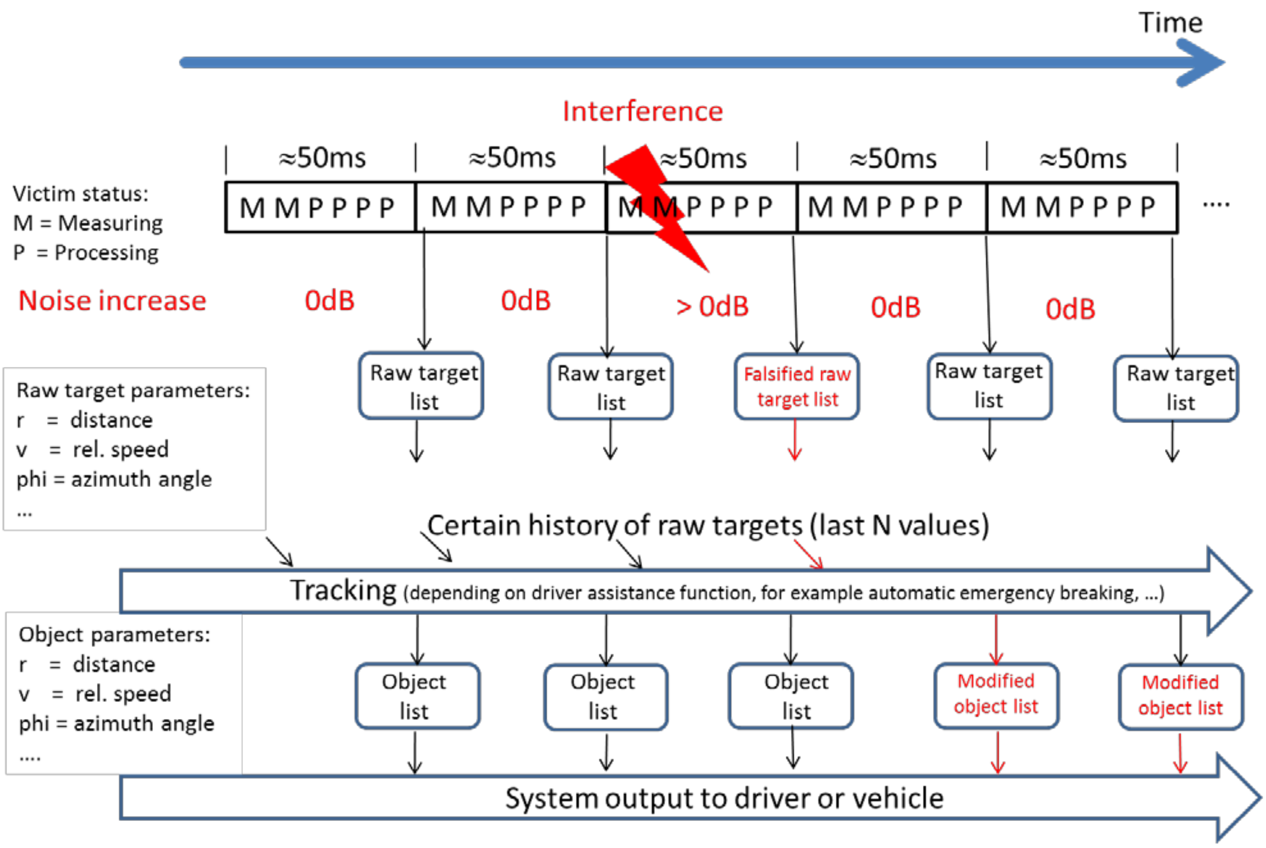


**Figure 56: Generalized overview on the operation of typical victim automotive radar sensors**

The end result of each cycle is a feature list (raw target list). The raw targets are then used in a tracking algorithm to obtain object lists. The tracking algorithm and the details of the object list are different from manufacturer to manufacturer and from application to application.

Furthermore, the interference will create different effects to the end user depending on the phase of the tracker when the interference occurs (see Table 26).

**Table 26: System level effects in automotive radar sensors where interference to cycles obscures a target vehicle or pedestrian**

| | Interference happens before a track has been initiated. | Interference happens when an object is already tracked for some time |
|---|---|---|
| **Interference to a single cycle only** | Formation of track and reporting of object is delayed, depending on track formation algorithms used. | Active safety features (e.g. emergency braking) may be temporarily disabled due to loss of raw target. |
| **Interference to several non-successive cycles** | Formation of track and reporting of object is delayed. | Impact to active safety features |
| **Interference to several successive cycles** | Formation of track and reporting of object is delayed. | Tracking of object is stopped and safety relevant feature is delayed. |
| **Interference to many successive cycles** | Sensor blind message | Sensor blind message |

The object lists are provided to an algorithm that produces the actual output signal to the driver or to the vehicle. The details of that algorithm are different from manufacturer to manufacturer and from application to application.

For comfort radar functions, a delayed reaction is perceivable to the driver.

For safety radar functions, delayed reaction is generally considered to be undesirable.

**Table 27: System level effects where interference is present on fixed infrastructure radar**

| | Interference happens before a track has been initiated. | Interference happens when an object is already tracked for some time |
|---|---|---|
| **Interference to a single azimuth or sector in a single scan** | Formation of track and reporting of object may delayed, depending on track formation algorithms used. | Tracker may coast but will not result in a dropped track |
| **Interference to a single azimuth or sector in non-successive cycles** | Formation of track and reporting of object or incident is delayed. | Tracker may coast and could result in track drop. Delay in reporting of objects or incidents |
| **Interference to a single azimuth or sector for several successive cycles** | Formation of track and reporting of object is delayed. Count and classify functions may be effected | Tracker will initially coast and then drop the track. Safety relevant features delayed. Possible false alarms |
| **Interference to a single azimuth or sector for many successive cycles** | Tracks will not establish and reporting of object is delayed. Count and classify functions may be effected | Tracks will be dropped close to effected azimuth or sector. Count and classify functions may be effected |
| **Interference to multiple azimuths in multiple sectors for many successive cycles** | Tracks will not establish. May result in non-detection of stopped vehicles or FOD. Safety relevant features delayed. Count and classify functions may be effected | Tracks will be dropped and false alarm rate will increase. Safety relevant features delayed. Count and classify functions may be effected |

- For statistical functions such as count and classify, interference has no safety related outcome;
- For safety radar functions, delayed reaction are generally considered to be undesirable;
- Increased false alarm rates due to interference are generally considered to be undesirable.

## 7.6 SUMMARY OF THEORETICAL STUDIES

- Interference is characterized by its power and time-dependency;
- Interference can cause noise increase or ghost targets;
- Noise increase can be rather uniform or structured;
- Consequence of noise increase strongly depends on victim details including detection history;
- Reduction of victim field-of-view in the order of 50% is possible.

# 8 MITIGATION MEASURES

**Table 28: Measures that could help to mitigate interference are discussed**

| Measure | Explanation of the measure |
|---|---|
| Limit the direct illumination time, for example by enforcing a fixed radar to scan mechanically or have duty cycle of <100% | The fixed radar considered in this report will directly illuminate a given point in space for an approximate period of 5 ms per second. At its nominal rotation rate of 4 times per second the illumination time is approximately 1.25 ms every 250 ms. This allows for a certain number of undisturbed automotive radar cycles. Non scanning fixed infrastructure radars need to have an equivalent duty cycle in time domain to achieve similar interference mitigation. |
| Select a scanning speed which avoids quasi-synchronous interference. Most automotive radars use a fixed measurement cycle time of 40, 50 or 60 ms | Depending in the design, the mechanically scanning fixed infrastructure radars may have a natural variation in rotation speed. It would be reasonable to expect a mechanically scanning fixed radar rotating at 4 Hz, as discussed in this report, to vary between 3.92 to 4.08 Hz or equivalent revisit time of 255 to 245 ms. This variance has been measured in an example system and is expected to be sufficient to avoid or reduce the probability of quasi-synchronous interference with automotive radars working on a 40 or 50ms measurement cycle. |
| Apply a small random offset to the automotive cycle times | Applying a random offset to the cycle start time (on the order of several milliseconds), would reduce the probability of establishing sustained period of quasi-synchronous interference between automotive radar and automotive radar, and between fixed infrastructure radar and automotive radar. However, there are limitations due to the synchronisation to the central vehicle bus. |
| Sector Blanking | Limiting the fixed radar to only radiating while in the direction of interest and not when outside the field of interest, would reduce the impact to automotive radars. This is termed Sector Blanking.<br>In order for the fixed radar to adequately detect, track and classify vehicles and reliably hold a given track identification to a particular vehicle then full coverage of all lanes is required. As described, limiting the transmission of power only to azimuths of interest to the Fixed infrastructure radar should be considered by the fixed infrastructure radar suppliers. |
| Switching off transmission of fixed and automotive radars when not sampling | In order to minimise the amount of interference produced in the band, it should be recommended that transmissions are only made when necessary. For example switching off transmission during fly-back or PLL settling time. SiGe and CMOS MMICs generally offer fast power switching. |
| Apply a level of jitter to the sweep start frequency | Applying a level of start frequency jitter between sweeps will help reduce the relative coherence between two or more radars. |
| Average Tx e.i.r.p. limit for fixed radar | The reduction of average Tx e.i.r.p. due to the mechanical scanning of the fixed radar showed an effective interference mitigation potential during the studies. |

# 9 CONCLUSIONS AND RECOMENDATIONS

This study has concentrated on radars using FMCW technology since those are the only examples made known to ECC during the course of the study.

For this study only one particular example of a fixed radar application has been investigated. This particular application has a main-beam peak Tx-Power of 39 dBm e.i.r.p., a detection range of ≤ 500m, a rotation frequency between 1 Hz and 4 Hz combined with 1.8° beamwidth at the 3 dB point and was tested at a mounting height of 4m. details as in [1].

On the automotive side, two examples of front looking radar sensors and one example of rear-side looking radar sensors from three different manufacturers have been investigated in this study. These have some features in common like using a kind of FMCW modulation or using a focussed antenna characteristics in elevation. But driven by different application requirements they differ in other features like transmit power, modulation bandwidth, antenna azimuth beamwidth or receive signal processing algorithms. More details on automotive radar sensors in general can be found for example in Recommendation ITU-R M.2057 [2] or in Handbook of Driver Assistance Systems [3].

This report has investigated scenarios with only one victim and one interfering sensor in an open area under ideal environmental conditions. The simulations are based on those assumptions.

This study analysed the impact:

- of one fixed infrastructure radar mounted at roadside installations used for road traffic monitoring onto automotive radar used for vehicle traffic safety and comfort functions;
- and automotive radars onto fixed infrastructure radar used for road traffic monitoring.

The study did not however investigate any impact of fixed infrastructure radar to fixed infrastructure radar systems or automotive radar to automotive radar systems.

The analysis was done based on

- detailed information on 3 different automotive radar systems from 3 different suppliers (Automotive Radar Systems A,B,C);
- detailed information on one fixed infrastructure radar system from one manufacturer;
- cooperative and organised experimental "open area" tests on the Neuhausen/Germany air field in a 1test campaign simulating typical roadside installation on highways (outside tunnels);
- simulations to verify the "open area" test results using a simulator based on the MCL (minimum coupling loss) method on spread sheet basis, developed during this work item.

In addition, two suppliers of automotive radar (systems A and C) independently tested the impact of an installation of 6 fixed radars deployed in the Hindhead/UK tunnel onto their automotive radar.

Both theoretical analysis and practical results show that the effect of any single FMCW radar on another operating at the same frequency is a raising of the post processing noise floor. This effect is the dominant one providing there is no accidental synchronisation between the two radars, which could increase the probability to detect ghost target. Due to movement of vehicles and scanning of fixed radar, the noise floor raising varies with time.

Establishing the exact degree by which the noise floor is raised and the overall effect on the radar is not straightforward. The theoretical model is the subject of debate and research; practical measurements are subject to a number of limitations. The following points, however, have been established:

1. The increases in noise floor (either calculated or observed) seen in this study can, be in the order of 10 dB or equivalent to a reduction of 45% detection range during an affected measurement cycle from a fixed infrastructure radar operating at 39 dBm, in certain scenarios based on particular radars and relative heights between radars.

2 Possibility of the noise floor increase depends on the probability of two or more systems with independent sweep parameters, scanning rate, occupied bandwidth and duty cycles illuminating each other during their transmit and receive period.

If a single typical vehicle radar passes a typical roadside infrastructure radar, then both radars will receive energy that may affect their operation.

The incident power received by the victim automotive radar from a fixed radar studied in this report at its antenna feed point can be of the same order of magnitude as the power received from a second automotive radar.

The simulation tool only calculates incident power levels at the victim's receiver antenna. Incident power alone does not directly transfer into interference. Incident power is only one aspect of interference being generated in the receiver. The simulation tool does not consider any system level or mitigation aspects beyond the receive antenna such as e.g. occupied bandwidth, frequency hopping, duty cycling.

The technical analysis in this report was set out to investigate worst case conditions for interference between the two radar applications in an open area roadside scenario. The analysis is not, however, representative of all real life installations.

Measurements and calculations from the limited analysis set out in Section 3 of this report suggest that:

- The impact of fixed radar onto automotive radar in open area is a transient (intermittent) and periodic 5-10 dB noise increase, resulting in a decreased sensitivity of the vehicle radar beyond the limit proposed by Recommendation ITU-R M.2057 [2]. This effect may appear above the system noise floor-level of automotive radars based on the probability of two or more systems with independent sweep parameters, scanning rate, occupied bandwidth and duty cycles illuminating each other during their transmit and receive period;
- The impact of automotive radars onto the fixed infrastructure radars in an open area is a transient (intermittent) and periodic noise increase. This may result in a decreased sensitivity of the fixed infrastructure radar in a given azimuth;
- With some evidence of increased impact in tunnels over open road scenarios, the exact effects could not be thoroughly studied due to missing propagation models.

However, with variations in radar types and specifications for both automotive and fixed radars, as well as variations in environmental layout, different simulation results could be reached.

The results of the analysis are detailed in the report in Table 29 below. However, recognising the limited analysis done and the fact that the test set-up conditions affect the coexistence, the correct approach to any further analysis needs to be considered carefully.

In summary, this report shows that, the scanning nature of the fixed installation radar contributes to the co-existence with automotive radars, as an interference mitigation method by:

- limitation in the illumination time as seen from a given point in space by the victim radar to ≤ 1,25 ms every 250 ms and ≤ 5 ms every 1000 ms, and;
- a silent time for undisturbed detection by automotive radar systems of no less than 240 ms every 250 ms. This can be achieved by limiting the re-visit time of the illumination.

The values above may need further consideration to take into account the different parameters.

**Table 29: Factors affecting coexistence between automotive and fixed scanning radars**

| Positive effect | Paragraph in the report |
|---|---|
| Small beamwidth of fixed scanning radar (Resulting in lower mean e.i.r.p.) | 2.4.2 |
| High Lateral and vertical separation of fixed scanning radar | 4.2<br>(may require further study) |
| Appropriate quality of silence time to reduce quasi-synchronous interference | 7.1.2 |
| Appropriate amount of silence time to ensure correct received signals by the automotive radar (Rotation of the fixed scanning radar) | 7.5<br>(may require further study) |
| Sector Blanking | 8<br>(may require further study) |
| **Negative effect** | **Paragraph in the report** |
| Reflections<br>(e.g. in tunnels, weather conditions) | 6.2.4<br>(may require further study) |
| Number of interferers<br>(only one interferer was studied in this report) | (may require further study) |

Finally, without known propagation models for road tunnels, it has not been possible to make an accurate prediction for compatibility. Therefore, further studies may be required before finally concluding on the tunnel case.

During the study it became apparent that the issues raised were far more complex than had been envisaged within the scope of this work item, which included differing vehicular radar types and implementations, different fixed radar mounting positions and configurations. This meant that conventional interference analysis was not considered possible.

## ANNEX 1: THEORETICAL AUTOMOTIVE RADAR BEAM PATTERNS

In order to simulate the different antenna diagrams for various type of radars and mounting positions, the following parametric approximation was used (taken from section 3.2.2 of Recommendation ITU-R F 1336 [6]):

$$G(\varphi,\theta) = G_{ref}(x)$$

$$G_{ref}(x) = G_0 - 12x^2 \quad \text{for} \quad 0 \le x < 1.152$$

$$G_{ref}(x) = G_0 - 15 - 15\log(x) \quad \text{for} \quad 1.152 \le x$$

$$\alpha = \arctan\left(\frac{\tan\theta}{\sin\varphi}\right)$$

$$\psi_\alpha = \frac{1}{\sqrt{\left(\frac{\cos\alpha}{\varphi_3}\right)^2 + \left(\frac{\sin\alpha}{\theta_3}\right)^2}}$$

$$= \varphi_3 \cdot \theta_3 \sqrt{\frac{(\sin\theta)^2 + (\sin\varphi\cdot\cos\theta)^2}{(\varphi_3\cdot\sin\theta)^2 + (\theta_3\cdot\sin\varphi\cdot\cos\theta)^2}} \quad \text{degrees}$$

$$\psi = \arccos(\cos\varphi\cdot\cos\theta) \quad \text{degrees}$$

$$x = \psi/\psi_\alpha$$

where

- $G(\varphi,\theta)$: gain relative to an isotropic antenna (dBi);
- $G_0$: the maximum gain in or near the horizontal plane (dBi);
- $\theta$: absolute value of the elevation angle relative to the angle of maximum gain (degrees);
- $\theta_3$: the 3 dB beamwidth in the vertical plane (degrees);
- $\varphi$: azimuth angle relative to the angle of maximum gain (degrees);
- $\varphi_3$: the 3 dB beamwidth in the azimuth plane (degrees).

The Figure 57 below represents the antenna diagram, for the follwing case: Gmax= 25 dB, 8° vertical FOV(at -3dB) and 15° horizonal FOV (@ -3dB). The scale of the colorbar is in dBi.

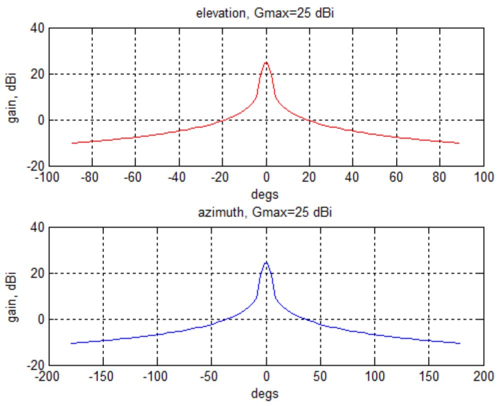


**Figure 57: View in the EL and AZ plane. View in the azimuth/elevation plane. Gain 25 dBi, vert. FOV 8°, horiz. FOV 15°**

The following figure represents the same diagram in the (azimuth, elevation) plane:

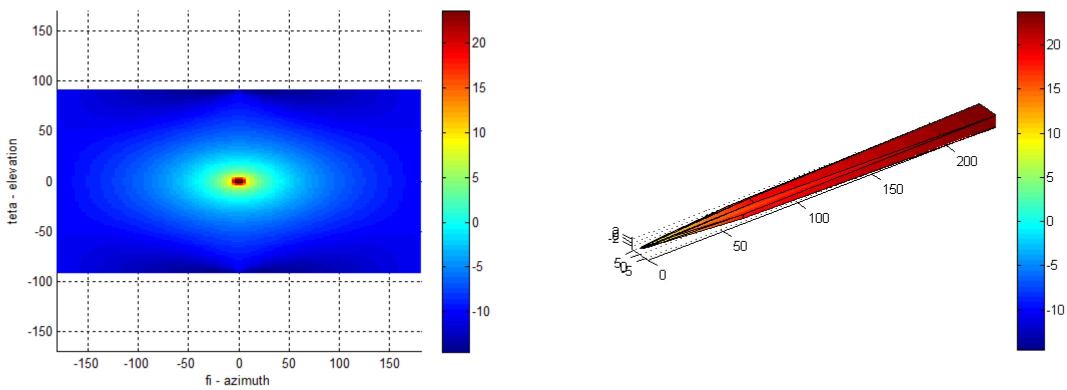


**Figure 58: View in the azimuth/elevation plane. Gain 25 dBi, vert. FOV 8°, horiz. FOV 15°**

The following figures are referred to an antenna with gain 10 dBi, 8° FOV in the vertical plane and 140° FOV in the horizontal plane. The scale of the colorbar is in dBi.

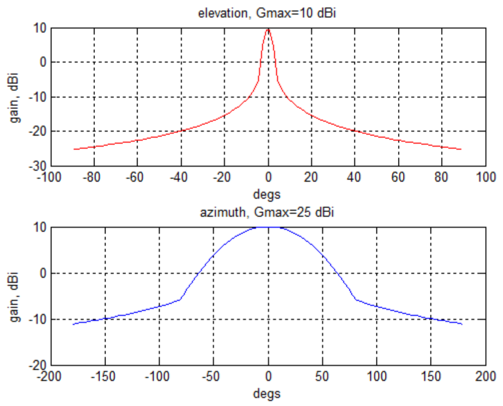


**Figure 59: View in the EL and AZ plane. View in the azimuth/elevation plane. Gain 10 dBi, vert. FOV 8°, horiz. FOV 140°**

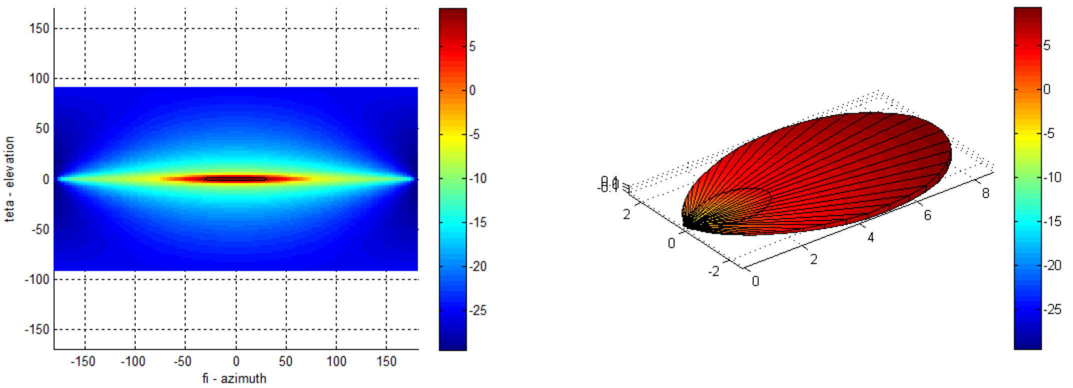


**Figure 60: View in the azimuth/elevation plane. Gain 10 dBi, vert. FOV 8°, horiz. FOV 140°**

## ANNEX 2: THEORETICAL DERIVATION OF AUTO-CORRELATION AND CROSS-CORRELATION

The following addresses the marked difference in response between an auto-correlated coherent signal return and a non-coherent cross correlated return in an FMCW radar and the significance of this to the interference performance.

Auto Correlation is simply defined;

$$F(t) = f(t + \tau) \text{ where } \tau \text{ is any defined period following t.} \quad (1)$$

Imperfect correlation is:

$$F(t) \neq f(t + \tau) \text{ for all or some periods } \tau \text{ after t.} \quad (2)$$

Auto-correlation is therefore dependant on the exact replication of the reference signal for all following reference periods, dependent only on the phase, $\phi$ between the reference signal f(t) and its delayed replica.

FMCW radar makes use of this property to generate a range beat frequency, proportional to range and the rate of change of the swept frequency range.

In the case of an absolutely linear frequency sweep and constant range, the range beat frequency demonstrates the same property of auto-correlation in the baseband – the frequency = constant and the amplitude is proportional to the distance,$1/ R^4$ of the target.

In the case of an interfering signal whose f(t) is not exactly coherent with the sweep frequency of the radar source, autocorrelation does not occur and instead we have cross correlation.

A simple definition of the energy spectrum of a signal W(ω) is:

$$W(\omega) = \text{(Power/Freq.Band)} = \text{power x time} = \text{energy E.}$$

This is simply defined for any signal that displays stationarity and ergodicity, such as Gaussian variation around a central frequency $f_0$. In the case of interference between two swept sources, $f_1(t)$ and $f_2(t)$ where the rate of change of signals, $f_1(t) \neq f_2(t)$ and $f_1 \neq f_2$ at t = 0, then correlation can only be partial in both the time and frequency domains.

If we consider the auto-correlation of a reference signal and a noisy version,

$$r(t) = s(t) + n(t) \quad (3)$$

where n(t) represents Gaussian noise modulation (random variance about a mean.), then the demodulation of the noisy signal depends on the sampling period t and the integration bandwidth, $\int f(t,\tau)$.

If we have a matched filter where the Gaussian variance is exactly covered by the integration bandwidth then we have captured the total energy in the signal r(t) and the output of the filter will be a steady state voltage.

If however, the variance is not matched by the integration characteristic, such as in the case of ‘white’ noise which has equal energy at all frequencies and is therefore ‘delta correlated’ (zero for all periods τ except τ = 0) then the integrated voltage must be very much less than in the first case. In auto-correlation, the result is the same as two CW signals at the same frequency fed into a mixer so that the only output is a DC voltage proportional to the phase difference between them. In cross-correlation, where there is no possible steady state, the signal can only exist as a transient, dependent on the relationship in both the time and frequency domains between the interfering signal and the swept source.

Therefore, interference between two sources depends on the temporal and frequency coherence between their separate functions, $f_1(t)$ and $f_2(t)$. The integrated level of the interfering signal is always less than that of a coherent return at the same power level, taking into account that an interfering source varies as $R^2$ and the radar return varies as $R^4$.

**Autocorrelation of a Linear FM pulse**

Given a modulated wave.

$a(t) = A(t) \cos \psi(t)$, then its autocorrelation function is;

$$B_a(\tau) = \int_{-\infty}^{\infty} a(t)a(t+\tau)dt \qquad (4)$$

Assuming only AM modulation (a pulse),

$a(t) = A(t) \cos \omega_0 t$, $\theta(t) = 0$, so that,

$A(t) = A^*(t) = A(t)$, then,

$$B_a(\tau) = 1/2\mathrm{Re}\,[e^{i\omega_0 t} \int_{-\infty}^{\infty} A(t)A(t+\tau)dt] \qquad (5)$$

Leading to, $B_a(\tau) = B_A(\tau)(\cos \omega_0 \tau /2)$

Where $(\cos \omega_0 \tau /2)$ is the autocorrelation of a harmonic wave of unit amplitude.

If we now carry out the same operation for a linear FM pulse, assuming perfect coherence, so that $\omega_{d1}\tau = \omega_{d2}\tau$ etc, then the autocorrelation function reduces to: (Ref 1)

$$B_a(\tau)/ B_a(0) = (\mathrm{Sin}\,[\omega_d \tau (1 - \tau/Ts)] \cos \omega_0 \tau) / \omega_d \tau \qquad (6)$$

where $B_a(0) = E$, the peak energy in the pulse.

$$= \mathrm{Sin}\,[(\omega_d \tau - \omega_d \tau^2/Ts)/ \omega_d \tau] \cos \omega_0 \tau \qquad (7)$$

We therefore end up with an equation relating the autocorrelation period $T_s$,
$\omega_d \tau$, the angular frequency of deviation WRT sample time and the auto-correlation of the harmonic wave cos $\omega_0 \tau$.
In the case of $\omega_{d1} \neq \omega_{d2}$, and $T_{s1} \neq T_{s2}$, then the interaction will be in the ratio of those two quantities for their individual cases.

The autocorrelation function of a linear FM pulse is plotted in Fig 2 and shows the classic sinc X/X form seen in the baseband of an FMCW radar.

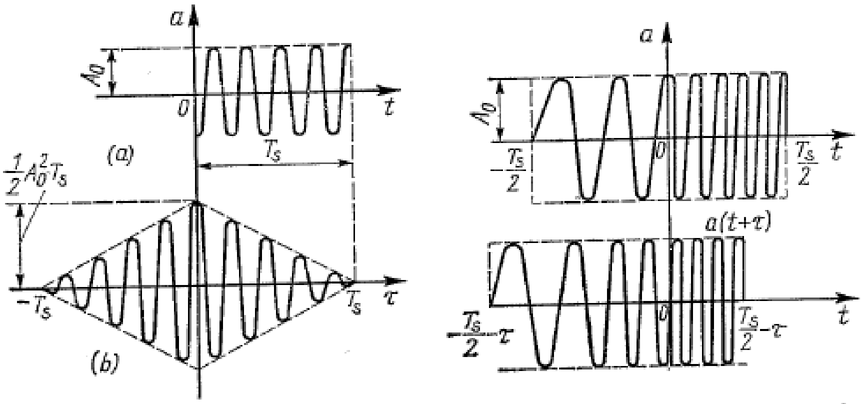

Fig. 3.27. (a) Pulse with a radio-frequency carrier and (b) its autocorrelation function

Fig. 3.28. Plotting the autocorrelation function of a linear FM pulse

**Figure 61: Autocorrelation of an RF pulse and the corresponding autocorrelation of a linear FM pulse**

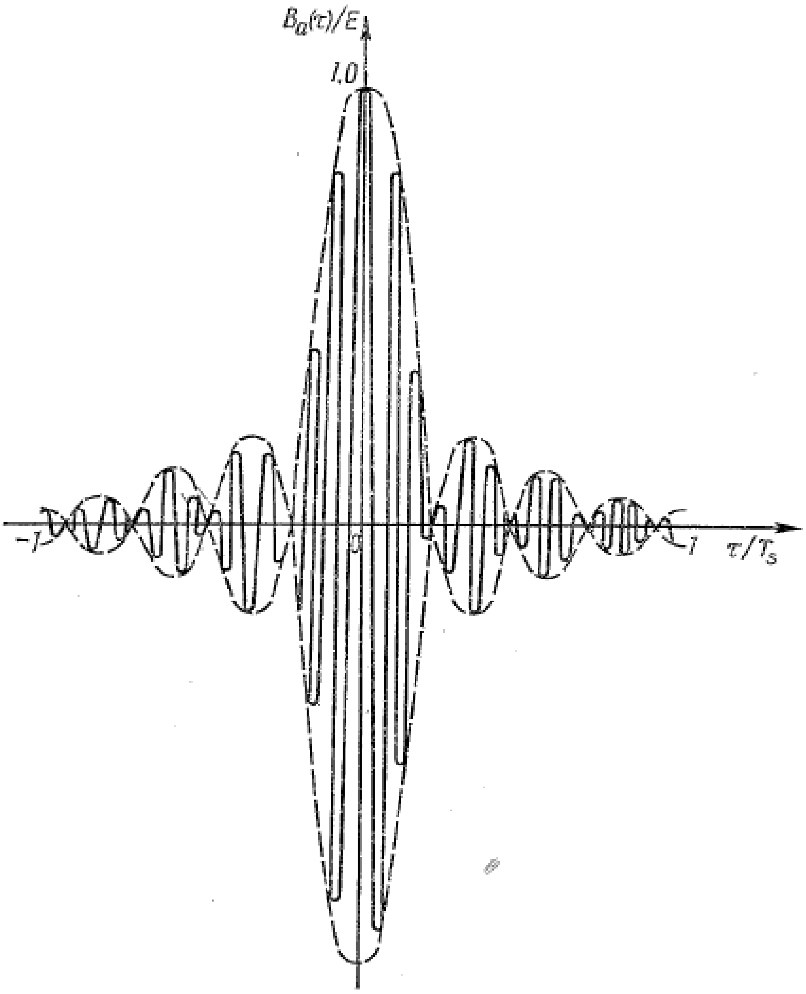

Fig. 3.29. Autocorrelation function of a linear FM pulse

**Figure 62: The autocorrelation function showing the compression of a linear FM sweep in the baseband of a FMCW radar**

### Cross Correlation

In the case of cross correlated signals, where coherence in either the frequency and time domain does not rigorously exist, the picture is much more complex. In the case of two signals, $s_1$(t), $s_2$(t), then the degree of cross-correlation is expressed by:

$$Bs1s2(\tau) \;=\; \int_{-\infty}^{\infty} s1(t)s2^{*}(t+\tau)$$

and for all real functions,

$$Bs1s2(\tau) \;=\; \int_{-\infty}^{\infty} s1(t)s2(t+\tau)$$

As is made clear in Ref 1, only in the case of even symmetry in the time and frequency domains, is there a direct correspondence in the symmetry of the cross- correlation. The peak of the correlated signal is not necessarily at the corresponding $B_a$(0) of either the interfering source or the victim.

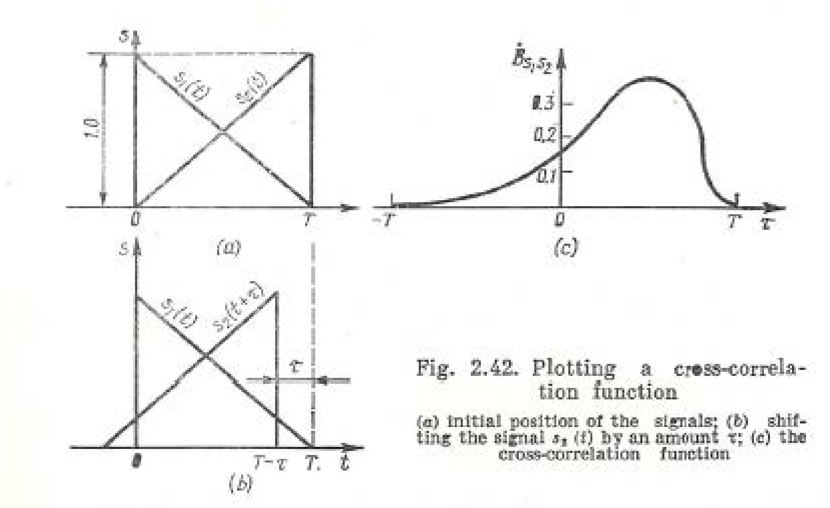


**Figure 63: Cross Correlation**

The result is that in the case of a swept FMCW receiver, the system has the greatest sensitivity to signals fully coherent with its own, in both the time and frequency domain. For all other swept interfering signals, within the baseband, the sensitivity is less and this sensitivity declines rapidly in both the time and frequency domain, larger the difference in sweep rate and relative frequency shift in the victim radar's passband, compared with its own correlated returns.

Therefore, for an accurate modelling of the level of interference between FMCW radars, their relative coherence must be included in the model when calculating the expected level of an interfering signal in the baseband of a victim radar.

## ANNEX 3: DEFINITIONS

**Coherence:** A qualitative term to describe the relative frequency ramp linearity, phase continuity and phase noise of any two transmitted FMCW signals.

**TRP**: Total Radiated Power (TRP): Integration of the power flux density of the radiated signal (e.g. e.i.r.p.) across the entire spherical surface enclosing the radar sensor under test

## ANNEX 4: LIST OF REFERENCES

[1] ETSI TR 103 148 V1.1.1 (2014-06), Technical characteristics of Radio equipment to be used in the 76 GHz to 77 GHz band; Short-Range Radar to be fitted on fixed transport infrastructur
[2] Recommendation ITU-R M.2057: Systems characteristics of automotive radars operating in the frequency band 76-81 GHz for intelligent transport systems applications
[3] H. Winner et al., Handbook of Driver Assistance Systems, Springer International 2016, chapter "Automotive RADAR" pages 325 ff.
[4] ERC Recommendation 70-03: Relating to the use of Short Range Devices (SRD)
[5] EC Decision 2013/752/EU: Commission Implementing Decision of 11 December 2013 amending Decision 2006/771/EC on harmonisation of the radio spectrum for use by short-range devices and repealing Decision 2005/928/EC
[6] Recommendation ITU-R F.1336: Reference radiation patterns of omnidirectional, sectoral and other antennas in point-to-multipoint systems for use in sharing studies in the frequency range from 1 GHz to about 70 GHz
[7] ERC Recommendation 74-01: Unwanted emissions in the spurious domain
[8] MOSARIM report “D16.1 – Report on interference density increase by market penetration forecast”, Section 4.3
[9] ETSI EN 301 091-1: Radar equipment operating in the 76 GHz to 77 GHz range